

Article

The Missing Link in the Genesis of the Lower Paleozoic Copper Deposits of the Anti-Atlas (Morocco): The Late Triassic Central Atlantic Magmatic Province Event

Mohammed Ouchchen ¹, El Hassan Abia ¹, Abderrahmane Soulaïmani ², Mohamed Abioui ^{1,3,*} , Brandon Lutz ⁴, Mohammed Benssaou ¹, Kamal Abdelrahman ⁵ , Tamer Abu-Alam ^{6,7,*} , Fatima Zahra Echogdali ¹ and Said Boutaleb ¹

¹ Department of Earth Sciences, Faculty of Sciences, Ibnou Zohr University, Agadir 80000, Morocco

² Department of Geology, DLGR Laboratory, Faculty of Sciences Semlalia, Cadi Ayyad University, Marrakech 40000, Morocco

³ MARE-Marine and Environmental Sciences Center—Sedimentary Geology Group, Department of Earth Sciences, Faculty of Sciences and Technology, University of Coimbra, 3030-790 Coimbra, Portugal

⁴ Rangefront Mining Services, Lode Metals Corp., Baker City, OR 97814, USA

⁵ Department of Geology & Geophysics, College of Science, King Saud University, Riyadh 11451, Saudi Arabia

⁶ The Faculty of Biosciences, Fisheries and Economics, UiT The Arctic University of Norway, 9037 Tromsø, Norway

⁷ OSEAN—Outermost Regions Sustainable Ecosystem for Entrepreneurship and Innovation, University of Madeira, Colégio dos Jesuítas, 9000-039 Funchal, Portugal

* Correspondence: m.abioui@uiz.ac.ma (M.A.); tamer.abu-alam@uit.no (T.A.-A.)



Citation: Ouchchen, M.; Abia, E.H.; Soulaïmani, A.; Abioui, M.; Lutz, B.; Benssaou, M.; Abdelrahman, K.; Abu-Alam, T.; Echogdali, F.Z.; Boutaleb, S. The Missing Link in the Genesis of the Lower Paleozoic Copper Deposits of the Anti-Atlas (Morocco): The Late Triassic Central Atlantic Magmatic Province Event. *Minerals* **2023**, *13*, 488. <https://doi.org/10.3390/min13040488>

Academic Editors: Huan Li and Han Zheng

Received: 26 January 2023

Revised: 25 March 2023

Accepted: 29 March 2023

Published: 30 March 2023



Copyright: © 2023 by the authors. Licensee MDPI, Basel, Switzerland. This article is an open access article distributed under the terms and conditions of the Creative Commons Attribution (CC BY) license (<https://creativecommons.org/licenses/by/4.0/>).

Abstract: Copper mineralization in the Lower Paleozoic sedimentary cover of the Anti-Atlas (Morocco) is continually being revised not only to improve its mining capacity, but also to determine its origin, which remains a matter of debate. As evidenced by the various models proposed, the related research is fragmented, localized, and confusing. The origin of the Anti-Atlas Lower Paleozoic copper mineralization is shared between synergistic and epigenetic processes or a superposition of the two processes. Based on new tectono-magmatic data and a reinterpretation of the ore structural arrangement, we propose a link between the last concentration of copper deposits and the Late Triassic–Early Liassic CAMP (Central Atlantic Magmatic Province) tectono-thermal event, as evidenced by the significant concentration of copper mineralization in the three NE–SW corridors affected by extensional faults, some of which are filled with dolerite CAMP magma. The heat flow generated by the mafic dykes within these reactivated corridors causes mineralized fluids to up well into the sedimentary layers, depositing material rich in juvenile or leached copper, or even a mixture of the two. In some cases, these fluids are trapped by fracture systems that accompany passive folds initiated on normal faults. In other cases, these fluids can infiltrate bedding planes, and even karst caves, formed during carbonate exhumation. Notably, extensive NE–SW faults systematically cover the early Hercynian structures, suggesting that they belong to a post-Hercynian extensional episode. During the Late Triassic, the global fragmentation of the Pangaea supercontinent was manifested by the stretching of the continental crust at the margin of northwest Africa, with the simultaneous opening of the Central Atlantic Ocean and emplacement of CAMP magmatism. This last and often overlooked tectonothermal event must be considered in the remobilization and reconcentration of copper mineralization and other mineralization in Morocco.

Keywords: copper deposits; Lower Paleozoic; Central Atlantic Magmatic Province (CAMP); Anti-Atlas; Morocco

1. Introduction

The Anti-Atlas area in east-central Morocco is known for its numerous copper mines, mineral resources, and copper deposits. Numerous archeological sites (slag, blast furnace

traces, etc.) have been exploited since the Middle Age [1,2]. The current increased demand and higher copper prices are attracting the greed of large-scale miners. From this perspective, a lot of geological mining and laboratory work is taking place. The National Geological Surveying and Mapping Program (PNCG), planned by the Moroccan Ministry of Energy, will allow for the elaboration of a geological platform based on detailed geological maps to accompany the exploration efforts.

In general, three types of copper mineralization can be distinguished on the Anti-Atlas scale: (i) volcanogenic massive sulfide (VMS) type exhalative deposits hosted in the Precambrian basement, for example, the Cryogenian Bleïda deposit in the Bou Azzer-El Graara inlier [3–6]; (ii) epithermal deposits associated with Upper Ediacaran andesite to rhyolite lavas (Alous, Assif n’Imider, and Issougri) [7–11]; (iii) epigenetic copper mineralization, the subject of this work, hosted mainly in the Lower Paleozoic cover (Tazalaght, Tizert, Jbel Laassel, Oumjrane-Bou n’Hass, etc.) [12–22]. Although a large number of copper deposits are operating or under development (Ouanssimi, Agjgal, Tazalaght, Tizert, Jbel Laassel, and Oumjrane-Bou n’Hass), in addition to a large number of artisanal and small-scale mining (Tasserirt, Imi n’Ifri, Talat n’Ouamane, Tadenst, Tiferki, Amadou, Tazert, Bou Skour, Asfalou, Akka n’Oulili, Bou Kerzia, etc.), only the Tizert site is eligible for large deposits with an estimated potential of 56,820,000 tons including 1.03% copper and 23 g/t silver [15].

The genesis of copper mineralization, hosted mainly in the Lower Paleozoic cover, is shared between the synergetic diagenetic and synsedimentary models [7,12–16] and epigenetic processes [17–22] or superposition of both syngenetic and epigenetic processes [7]. Nonetheless, there is consensus that the Upper Ediacaran basement, composed of volcanic, volcanoclastic, and intrusive rocks, represents a likely source of copper, as evidenced by the andesite and rhyolite lavas of Alous, Assif n’Imider, and Issougri [7–12].

The synergetic diagenetic and synsedimentary models suggest that the Early Cambrian organic-rich sedimentary sequence represents a chemical trap of disseminated copper sulfides. These first deposits from the first Cambrian transgression filled a system of depressions bounded by emerging paleohighs. This paleogeography was caused by a volcanism-rich rifting in the Upper Ediacaran, which appears to have continued into the Lower Cambrian [23].

Instead, the presence of a different type of sulfide mineralization, typified by copper-filled fractures and veins, with the same mineralogical signature as the disseminated deposits, supports the epigenetic model [21]. The timing of these copper occurrences is still debated, although most works mention Hercynian compressions [15–22].

In general, a common feature of the Lower Paleozoic copper deposits in the Anti-Atlas is that they all have simple mineral assemblages including hypogene assemblages of bornite, chalcopyrite, and incidental pyrite as well as supergene assemblages with a copper-rich mineral phase, native copper, chalcocite, covellite malachite, and azurite. Except for the Bou Skour deposit and some localized occurrences in the Tamjout Formation, there are little or no lead and zinc sulfides. These sulfides should not be confused with the galena and sphalerite found in the deposits that form the lead-zinc belt around the Anti-Atlas copper area: the Jbel Jaouad and Bou Lbaroud deposits in the west, the Addana vein in the south, and the eastern deposits in the Ougnat and Tafilalt areas in the eastern Anti-Atlas [24] (Figure 1).

This paper aims to elucidate the genesis of the controversial Lower Paleozoic copper mineralization based on new structural data and a reinterpretation of the aspects of the ore texture. We emphasize the importance of the last significant tectonothermal event experienced by the Moroccan continental crust during the Late Triassic, coinciding with the opening of the Central Atlantic. Indeed, this oft-overlooked extensional event, characterized by CAMP (Central Atlantic Magmatic Province) magmatism, had a considerable impact on the remobility and reconcentrations of copper deposits along the identified activating corridor. To achieve these objectives, we first present a synthesis of the regional geology and the geology of the mineralization in question, highlighting the problem of their

southwestern parts are composed of Eburnean low-to-medium grade metamorphic units, intersected by many granitoids at around 2Gy. The Eburnean basement is covered with a large unconformity by Neoproterozoic Pan-African terrains that range from the Cryogenian to the Ediacaran or directly by the Lower Cambrian transgressive series.

After a prolonged quiescence through the Mesoproterozoic, except for some mafic dykes that bisected the Eburnean basement [33–35], the Precambrian deposits resumed with the Pan-African cycle by a large platform (Bleïda Tachdamt Group) established on the northern edge of the West African Craton (WAC). Coincidentally, oceanic lithosphere and magmatic arcs developed northward [31]. Various rocks of this Neoproterozoic setting were stacked along the Anti-Atlas Major Fault corresponding to the Pan-African suture during several Pan-African accretions from 750 to 640 Ma [36–38]. The paroxysm of the Pan-African orogeny was marked by the emplacement of syntectonic quartz-diorite plutons along the Bou Azzer suture at around 650 Ma [39]. The Ediacaran siliciclastic and volcanoclastic deposits underline the waning stages of the Pan-African orogeny.

The carbonate-dominated Adoudou and Lie-de-vin Formations [40,41] unconformably overlie the Precambrian rocks, forming the Ediacaran–Cambrian transition and beginning a long and continuous Paleozoic sedimentary cycle. The Paleozoic sedimentary cover of the Anti-Atlas, ranging in age from Cambrian to Carboniferous, is thicker in the southwest (about 10,000 m) and less than 6000 m in the east [25,42]. It rests paraconformably or with angular discordance on the Ediacaran volcano-sedimentary sediments of the Upper Ediacaran Ouarzazate Formation (Figure 1).

The Cambrian formations, deposited in a rifting context [43,44], are divided into three lithological groups: the Taroudant Formation, the Tata Formation, and the internal Feijas Formation. The Taroudant Formation (Adoudounian) sedimentary sequence shows two units, the carbonated “Oued Adoudou” or “Adoudou Formation” [45] and the Taliouine Formation, formerly known as “Lie de vin” [46]. The Adoudou unit is divided into a lower unit called the “Series de base” and an upper unit called the “Lower Limestones” [40]. The “Serie de Base” consists of a trilogy, usually from a conglomerate top covered with lower limestone [47] to the end of a silty clay interval [43,48,49]. The series is well-represented in the western Anti-Atlas (400 m) and thins rapidly eastward, disappearing in the central Anti-Atlas. The lower limestone begins with the prominent silicified Tamjout dolomite layers, which are topped by stromatolite dolomite sequences. These later were intruded in the central Anti-Atlas by the Alougoum trachyte lava flow, dated at 534 ± 10 Ma (U/Pb on zircon) [50,51]. The Taliouine Formation consists of dark red argillaceous rocks intercalated with carbonate layers [52], which are gradually becoming terrigenous toward the central and eastern anti-Atlas regions to form the Tikirt sandstones [53].

Following the Taliouine’s terrigenous series, the Tata Group highlights the deposits of the “upper limestone” or Igoudine Formation, consisting of massive carbonate layers intercalated with grey siltstone. The latter thickens at the expense of carbonate and accumulates vertically in the sandstone, forming the “Slate limestone Formation” or “Amouslek Formation” [40,54].

The “Feijas interne” Group consists solely of siliciclastic deposits called “paradoxides schists” [55,56], which are silty-clay deposits with massive sandstones that form well-individualized quartzite cuesta in the central Anti-Atlas, known as the Tabanit Group [57].

The Ordovician consists of a thick silicoclastic series divided into four lithostratigraphic groups: (i) the External Feijas Group, (ii) the 1st Bani Group, (iii) the Ktaoua Group, and (iv) the 2nd Bani Group. External Feijas and Ktaoua Groups are mainly composed of clay, while the 1st Bani and 2nd Bani groups are mainly composed of sandstone [58,59]. The Silurian is clay in nature but has very typical sandstone and *Orthoceras* limestone layers [60]. Above, the Devonian consists of shale, black *Orthoceras* limestones, and reef limestones [26]. The Carboniferous includes sandy-calcareous beds and green shales [61].

During the Late Carboniferous, the Anti-Atlas area experienced Hercynian orogeny, forming the foreland fold belt of the Meseta Block to the north and the Mauritanides to

the southwest [42,62,63]. Precambrian basement faults were reactivated and the Paleozoic cover was slightly folded [24,25,42,64,65].

The Mesozoic–Cenozoic evolution of the Anti-Atlas is ill-established due to the lack of related deposits along the Anti-Atlas chain. Several NE–SW Lower Liassic mafic dykes belling to the CAMP magmatic event crosscut the entire Anti-Atlas, indicating the Triassic rifting of the supercontinent Pangea at the Triassic–Jurassic boundary [66,67]. Let us recall here that the CAMP is one of the largest igneous provinces (Large Igneous Provinces, LIPs), where a large quantity of magma has appeared, in the form of doleritic sills and dykes and basalt flows, on the three African continents. The European and American united in Pangea 200 Ma ago [68–70]. These provinces are often associated with the formation of metalliferous deposits, in particular, ortho-magmatic Ni-Cu-Co-PGE [71], and can also influence the formation of hydrothermal deposits; the thermal flux brought by the magma would cause hydrothermal convection, which will mobilize the metals of magmatic origin and/or are leached by percolating through the basement, then migrating toward the surface along the extension faults.

After periods of burring and exhumation, the Anti-Atlas acquires its current topography during the Neogene, contemporary to the Alpine High Atlas uplift [68–72].

In the early Mesozoic, the Anti-Atlas area served as the southern shoulder of the Atlas rift, coinciding with the opening of the Central Atlantic. At this time, the Anti-Atlas crust was stretched and affected by extensive faults, which are superimposed on the Hercynian structure, as shown in the eastern Anti-Atlas [73].

3. Materials and Methods

The fieldwork focused on (i) the mapping at a detailed scale of the main copper deposits, (ii) the characterization of the kinematics of the Triassic-Liassic rift that controlled the emplacement of mineralization, and (iii) the production of a textural description of the ore at the scale of the outcrop. The prominence of the basement normal faults that do not cross the entire Paleozoic cover is supported by relief dynamics studies approached from geomorphological markers such as alluvial fans or triangular facets.

In the laboratory, sections and prepared polished blades were polished until obtaining flatness and perfect polishing. For blades, the optimum thickness was around 25 μm . Subsequently, they were examined and analyzed microscopically, which makes it possible to fine-tune the textural aspects of the ores.

The magnetic data used were acquired during a helicopter-borne geophysical campaign in the Moroccan Anti Atlas in 1999, carried out on behalf of the Ministry of Energy and Mines by the company Géoterrx-Dighem. The acquisition was made using a Eurocopter AS350B2 and AS350B3 type helicopter, equipped with a video recording system (PAL video camera). The flight lines were oriented N15° to N315° and spaced 500 m apart. The measurements were taken with an average ground clearance of 30 m using a Scintrex Cesium or Geometrics-type magnetometer with a sensitivity of 0.01 nT. These data were subject to corrections corresponding to: (i) denoising by noise elimination, (ii) elimination of closing errors, and (iii) corrections due to diurnal variations. The residual data were transformed, so that the magnetic anomalies appeared at the right of the magnetic sources, using a “reduction to the magnetic pole” (RTP) operator using a magnetic inclination of 41.1° and declination of 4, 5°.

4. Western Anti-Atlas Copper Mineralization along the Igherm Ridge

The western Anti-Atlas morphostructure is dominated by a succession of NE–SW to N–S Hercynian synclines (Issafène, Talat n’Yissi, and Ouansimi), affecting the Paleozoic series between the basement uplifts of the Ifni, Bas Drâa, Kerdous, and Igherm inliers, which form the core of the adjacent anticlines [22,25,63,74] (Figure 2a). Western Anti-Atlas was first mapped by a 1/500,000 scale geological map and then by 1/100,000 scale geological maps of Tiznit, Tafraout, Taroudant, and Igherm [74–78]. Precambrian basement outcrops were of particular interest during the PNCG program by producing 1/50,000 scale geological

maps (BGS, BRGM). Most of the western Anti-Atlas copper deposits are located along the NE–SW line between the Ouansimi deposit south of the Kerdous inlier and the Igherm area, interestingly highlighting the direction of the great Igherm dyke, which is part of the CAMP (Figure 1).

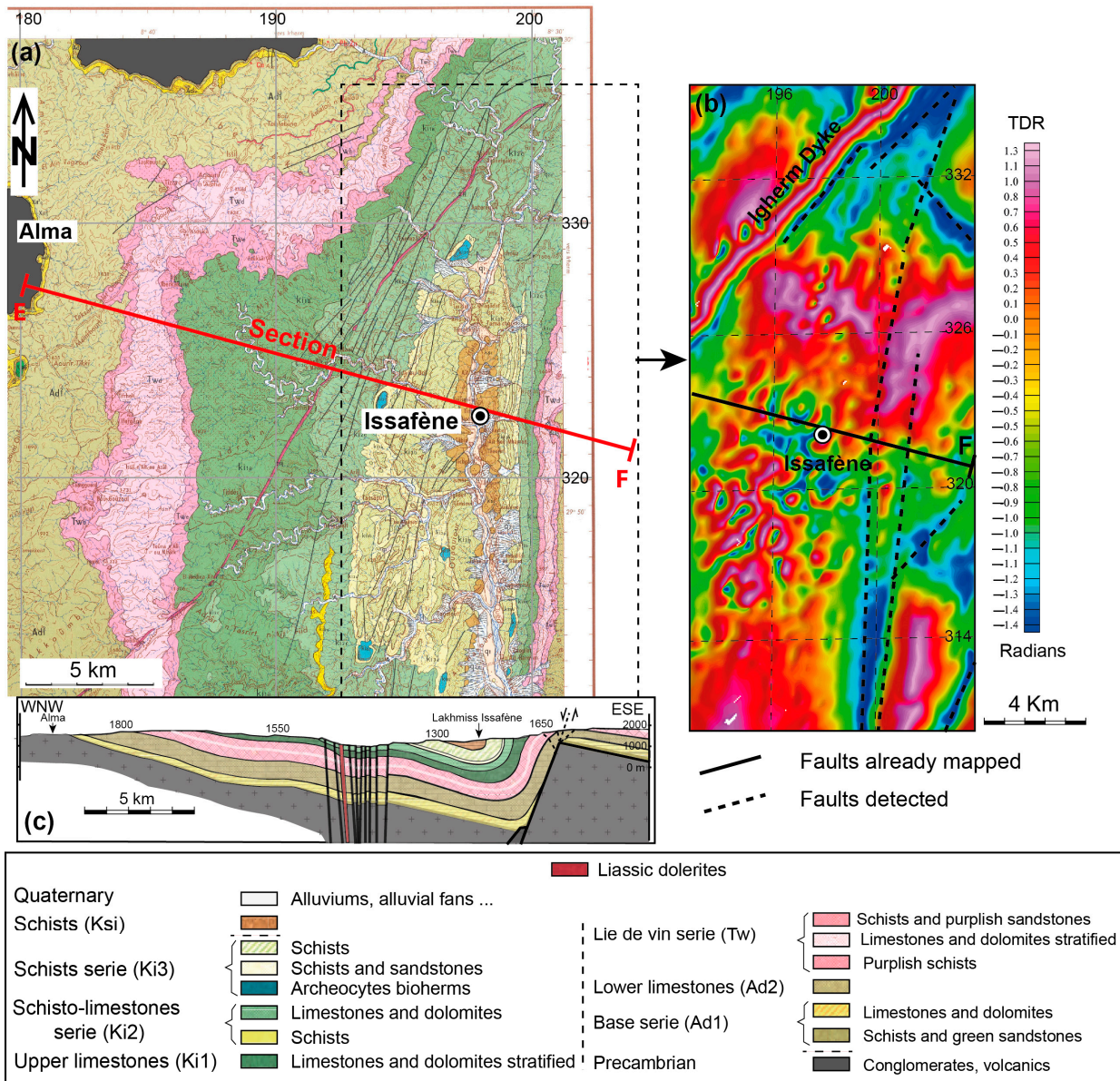


Figure 2. (a) Geological map of the Issafène syncline (excerpt from the Tafraout geological map at 1/100,000). (b) Map of the residual magnetic field transformed by the “derivative tilt” method of the Issafène region. (c) Interpretive geological cross-section (cross-section E-F on a map in Figure 1a).

4.1. Morphostructural Considerations of the Issafène Syncline

A broad cliff slope of more than 30 km is formed on the east side of the north–south Issafène syncline, along which triangular facets and alluvial cones can be seen (Figure 3). The formers develop there in a repetitive fashion, alternating with the flow of “talweg” perpendicular to the embankment. Sediments that reach the estuary are deposited in the form of alluvial fans. Triangular facets provide good morphotectonic markers for the relative interactions of the underlying blocks; they arise from the gradual exhumation along normal faults [79–81]. According to these authors, the topographic differential created by

the fault motion leads to erosion of the footwall, and incisions are concentrated on major drains that delineate interfluve zones where the topography is better preserved.

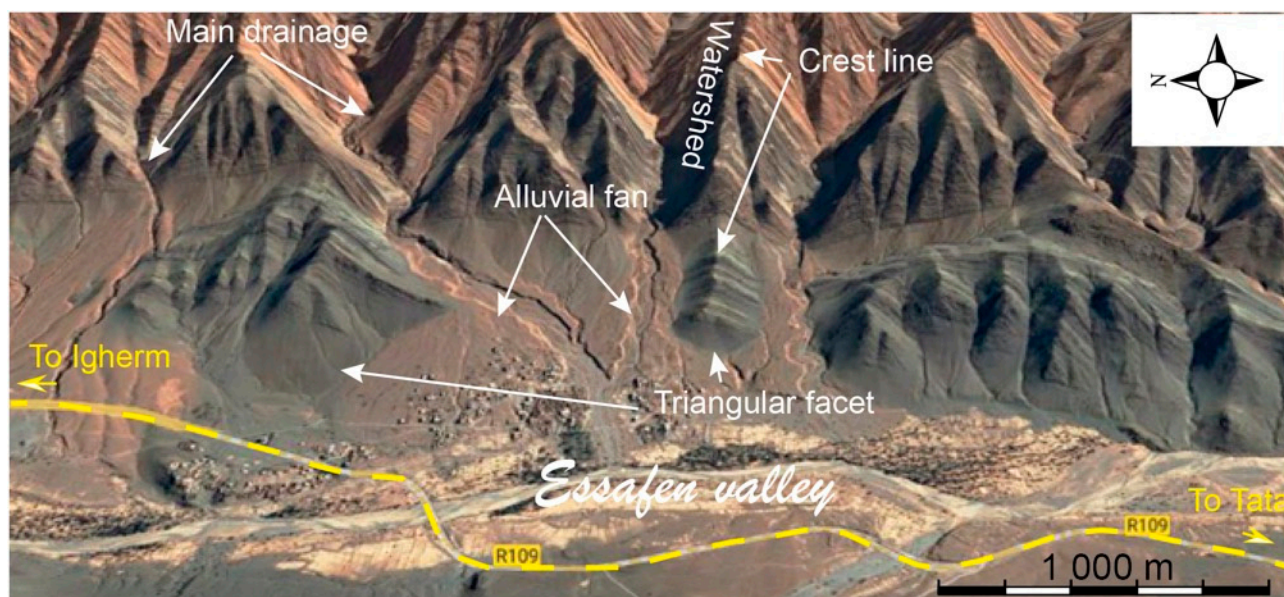


Figure 3. Morphological markers developed along the Issafène escarpment (Google image).

A geological cross-section transverse to the Issafène syncline axis shows that it is an asymmetric fold with a SSW–NNE axis with a near horizontal plunge (Figure 2c). Its east side straightens vertically, while its west side slopes slowly toward the opposite boundary. The adjacent eastward anticline is also asymmetric, with its west side common with the syncline while the east side appears as slightly sloping to the east with no more than 20° . This disposition draws knee fold with the extrados affected by a dense fracture parallel to the axis. It appears as slightly open joints, vertical crevices filled with quartz, carbonates of Ca and Fe (calcite and ankerite), oxides and hydroxides of iron, and traces of copper, microscopic copper in the form of malachite and rarely azurite, microfaults and overlapping shears between striated beds. In some places (N $29^\circ 51' 42.78''$; W $8^\circ 30' 17.57''$), the fractures were so strong that the rock (lower limestone) took on the appearance of breccia. Away from this joint, the fracturing intensity diminishes rapidly and re-emerges cautiously westward, where a set of normal faults and the Iggherm dyke run in the same direction across the entire Cambrian cover.

The asymmetrical layout of the Issafène syncline is often interpreted as a western Hercynian vergence, which is inconsistent with the known western Anti-Atlas global SE vergence [25]. This asymmetrical anticline is unique on the scale of the western Anti-Atlas, and its geometry is reminiscent of the Rattlesnake Mountain Anticline (Wyoming, USA), which is developed in an extensional regime directly above an underlying rigid bedrock fault [82], and thus likely to be linked to the same context of a post-Hercynian crustal extension. As suggested by the very steep dip of the east flank, a basement fault governing the Issafène fold should have been sub-vertical. The fact that this fault does not cut the entire sedimentary cover can be explained by the extensional Trishear model. Furthermore, the interpretation of aeromagnetic data favors the rationality of this hypothesis. A map of the residual magnetic field in the Issafène region transformed by the ‘differential dip’ method highlights a linear magnetic anomaly (Figure 2b): a very strong anomaly that perfectly matches the Iggherm and other database dykes, with low intensities corresponding to the NW–SE, N–S, and NE–SW trending faults, some of which have been plotted in situ, while others are not assumed. This extends over 20 km in the NNE–SSW direction.

In all of these respects, this fold developed in an extended region over a rigid bedrock fault, providing an ideal model for the emplacement of copper mineralization. To better

illustrate this formation model, in the paragraphs below, we develop examples of the Ouansimi and Tazalaght deposits, which are part of the Igherm Ridge, to the south and east of the Kerdous inlier, respectively.

Located south of the Kerdous inlier, the Ouansimi deposits at the mine level, the Adoudounian series with copper mineralization, overlie the Ouarzazate Group clastic deposits with a transgressive ravinement surface. It consists of alternating sandstone and siltstone interbedded by limestones of “Serie de base”, followed by the “Lower Limestones” of the Adoudou Formation, which begins with the massive Tamjout dolomite and ends with the layered dolomitic limestone. The Taliouine Formation is a series of dolomite formations interlayered by red marl. The Amouslek Formation, or “Upper limestone”, terminating the Paleozoic series, depicts an asymmetric fold with an N 45° E subhorizontal axis (Figure 4b). Its straightened northwest flank (70 to 90°) contacts the Precambrian bedrock and gradually flattens over a few hundred meters. On the other side, however, the layers are only slightly (20°) inclined toward the southeast.

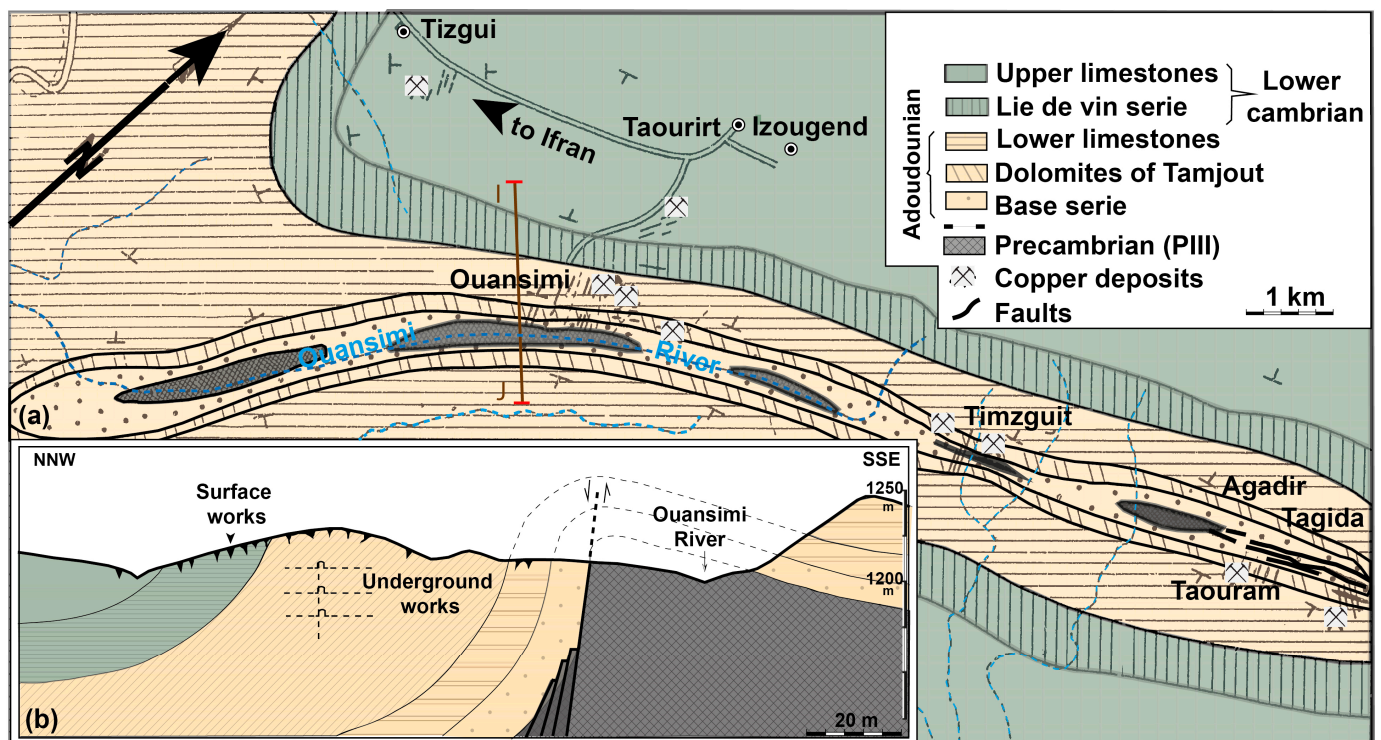


Figure 4. (a) Geological map of the Ouansimi district. (b) Geological cross-section I-J (modified after Smeykal [22]).

The folded structure is accompanied by a network of fractures, most evident in the Adoudounian limestones, which can be subdivided into the axial fracture type and transverse fracture type. The first family is represented by joints slightly oblique to the bedding, calcite-quartz-filled fractures, and sliding joints parallel to the bedding that are highlighted by ripples on the joint surface. Intersecting fractures affecting all folded units including the Upper Ediacaran Ouarzazate Group are particularly rich in copper mineralization. The intersecting fractures are sub-vertical (>70°), with evident decimeter to metric vertical offset along the entire northern flank, and they are visible from more than 300 m of the fault contact with the Precambrian substrate. There, mineralization developed as a network of small veins that are several meters wide. Sometimes it is deposited laterally along bedding surfaces and slip planes, giving the ore body a layered morphology [22]. The ore consists of copper sulfide in quartz-carbonate gangue.

4.2. Tazalaght Site

Further northeast, about 150 km southeast of Agadir on the eastern edge of the Precambrian Ait Abdallah inlier, the Tazalaght deposit (N 29°45'6.89"; W 8°43'23.91") lies on a folded structure about 500 m along the NNE–SSW axis. The lower part is the conglomerate of the Upper Ediacaran Ouarzazate Group, above which are the siliceous deposits “Série de base” Formation, followed by the Tamjout dolomite. The Ediacaran conglomerate overlies the Paleoproterozoic basement quartzites unconformably and is locally absent, in this case, the “Série de base” Formation occurs directly in fault contacts with the Precambrian basement (Figure 5).

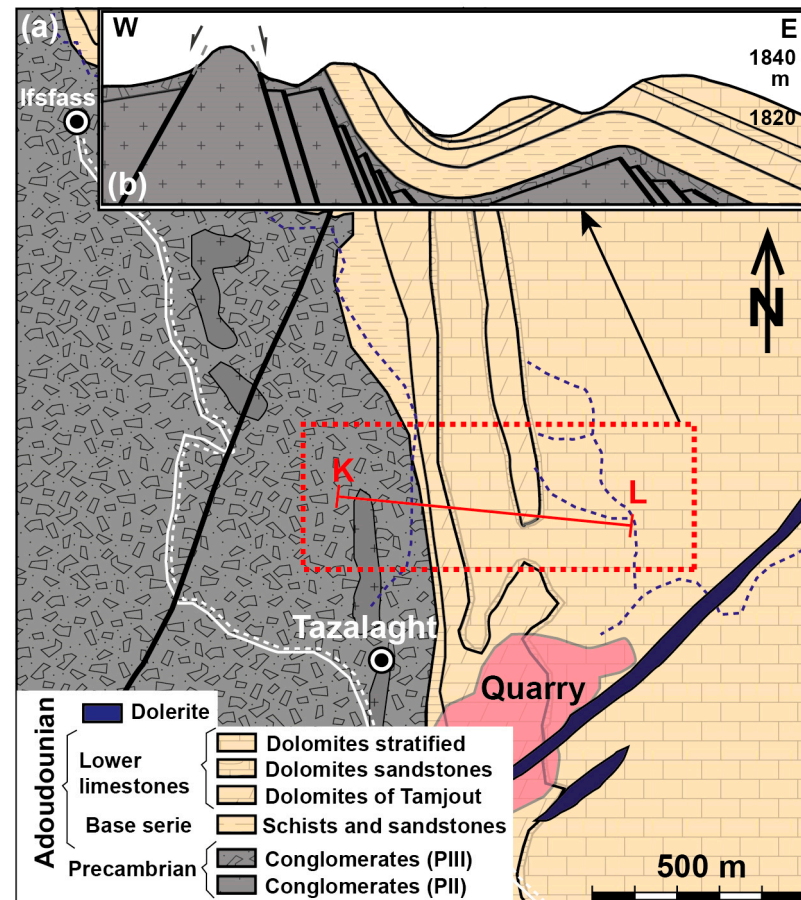


Figure 5. (a) Geological map. (b) Section K-L of the Tazalaght mining site (modified from El Basbas [20]). PII: Precambrian II. PIII: Precambrian III.

Structurally, the Lower Paleozoic series and its Precambrian substrate are affected by Hercynian and post-Hercynian deformations [73,74]. At the lower levels, especially within the limestone units, many small drag folds flow eastward. The sliding of competent limestone layers on the interlayered plastic siltstone levels caused these typical Hercynian folds. These Hercynian folds belong to a regionally asymmetric fold structure, with the western flank in contact with the basement fault being strongly straightened (dip >70° eastwards), while the opposite flank is approximately 400 m long and slopes slightly westward (Figure 5). This fold is connected to another syncline of the same shape to the east. These folds are associated with brittle structures distributed in two principal directions, NNW–SSE and NNE–SSW and NE–SW. The first trend is represented by a series of sub-vertical normal faults that significantly affect the basement, which along with other fractures, host mineralization in the form of veins and stockwork. In the sedimentary cover, these extensive faults induced the same folds that are observed at the mine level. In addition to the mineralization outlined below, the most abundant areas are located at the top of the

“Série de base” Formation, preferably along contacts that define high-contrast lithology or those that favor detachment levels. Along the detachment plane, the ore exhibits a laminar appearance parallel to the bedding [7,15,83–85], reminiscent of the texture of the syngenetic deposit. In the carbonate facies, mineralized veins sometimes exhibit layered diverticula, forming stratiform clusters characteristic of Mississippi Valley-type (MVT) mineralization.

5. The Central Anti-Atlas Area and Associated Mineralization

The central Anti-Atlas consists of an Eburnean basement formed of metasediments (gneisses, amphibolites, micaschists) intruded by a succession of granitoids, topped in major unconformity by the Neoproterozoic, which includes an ophiolitic complex and a range of sedimentary deposits ranging from continental and platform environments with flyschoid facies often associated with effusive tholeiitic volcanism, injected with calc-alkaline granitoids and a network of basic dykes (dolerites and gabbros) dominated by continental tholeiites [24,30,32,34,35]. These units are structured during the Pan-African orogeny in the greenschist facies [24]. Next, come and in unconformity, the volcano-sedimentary terrains of the Ouarzazate Super Group (late Neoproterozoic), which are made up of a succession of ignimbritic sheets occasionally intercalated with flows of rhyolites, andesites, basalts, and sedimentary deposits [41]. The Paleozoic cover is weak in this region: the Adoudounian is reduced to its maximum and the basic series is lacking [46]. All of these lands are crossed by the large Fom-Zguid dyke attributed to CAMP [66].

5.1. Structural Data

In the central Anti-Atlas, the Hercynian trend of the Paleozoic folds is more complex by the long axis of the Bou Azzer-El Graara inlier, which runs from northwest to southeast. Leblanc [86] distinguished several drag folds, fan-shaped, conical, and more or less inverted, attributed to the Hercynian orogeny. These folds are the result of thick-skinned tectonics, which reactivated old fractures [28,87].

Pot-Hercynian deformations are characterized by brittle faults, some of which exhibit extensive offset, often in clusters. Note the presence of a swarm of CAMP-doleritic dykes, most importantly the NE–SW Fom-Zguid great dyke, which intersects the Bou Azzer-El Graara inlier. Numerous copper deposits have been reported in the area at the bottom of the Paleozoic cover, the most important of which is undoubtedly the Jbel Laassel copper deposit, which we will describe in detail after a brief structural description of the Paleozoic cover.

In the central part of the Anti-Atlas, in addition to the NE–SW Lower-Liassic dyke [88], the Paleozoic sedimentary cover is affected by a network of faults organized along two main directions: N 20° to N 30° and N 60° to N 70°; the latter direction is the most common (Figure 6). Taking the geological section south of the Bou Azzer-El Graara inlier as an example, some faults have a normal offset such as the F3 fault, which contacts the Lower Cambrian and Lower Ordovician [89]. These are consistent with the NW–SE extension with the vertical principal stress axis σ_1 . Others do not affect the entire Paleozoic cover such as F4, which truncates the Lower Cambrian and disappears in the Middle Cambrian, leading Emran and Chorowicz [89] to consider these types of faults to be synsedimentary faults. In our opinion, the upward die-out of some normal faults can be explained more simply by the extensional three-shear model, as previously described in the Igherm area.

The N 20° to N 60° directions correspond to fracture fields (tension-gashes structures) filled with quartz, Ca and Mg carbonates, and iron oxides and hydroxides, with occasional traces of copper associated in the form of malachite.

5.2. Jbel Laassel Deposit

The Jbel Laassel deposit occurs along the axis of a ~2 km-long NE–SW fold within the dolomites of the “Upper limestone” Formation [19]. At both ends, the fold axis is horizontal and then slightly inclined (<20°) toward the center of the structure, influenced by a NW–SE fault. Its steepest north flank is bounded by the NE–SW fault, while the other flank slopes slightly toward the northwest (Figure 7). This latest accident is reported by Bourque et al. [21]

as a thrust fault. However, at strong dips, as indicated by the very steep dips of the flanking formations in the tectonic contact, it should have instead been a set of near-vertical faults with a normal offset that control sedimentary cover subsidence by forming folded structures intruded by dolerite dykes similar to those of the Foug-Zguid area.

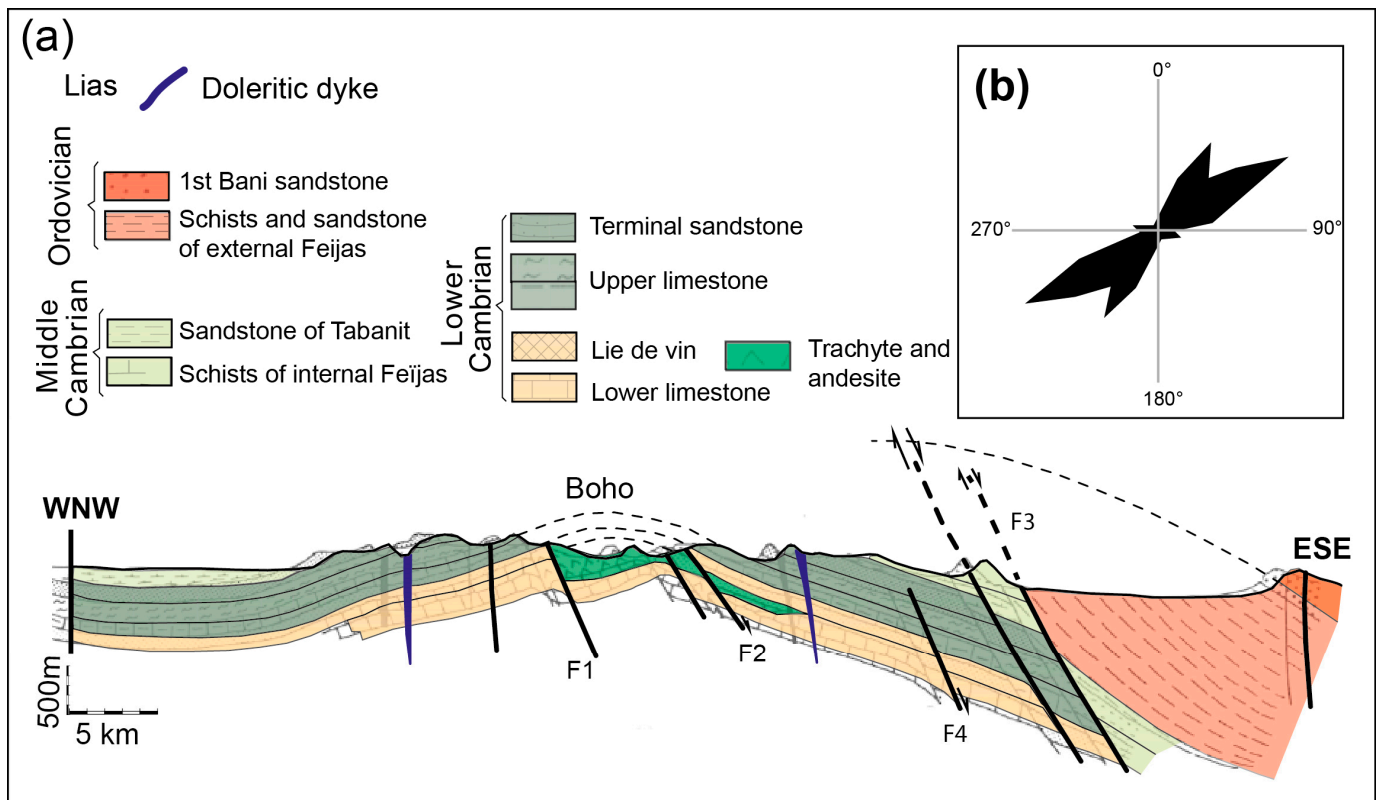


Figure 6. (a) Geological section of the Foug-Zguid area (E-F section in Figure 1). (b) Rosettes of cumulative length-weighted frequencies of fractures recorded on Landsat MSS space images for the Cambrian identification of the pushover of the eastern and southern edges of the Bou Azzer-El Graara inlier (adapted from Emran and Chorowicz [89]).

The NE–SW syncline that dominates the regional landscape is superimposed by a regional fold system with the NW–SE direction “Ougartian trend”, with a straight axis, and a 25° NW oblique axis [6,21]. The formation of the Jbel Laassel syncline structure was accompanied by secondary fractures, microfolds, and slip planes. On the fold hinge, intersected by the NW–SE accident, over an area of approximately 150,000 square meters, interwoven fractures form a coherent network of thin veins filled with copper ore containing quartz veins and calcite. Disseminated mineralization was observed in a calcareous mass of the host rock.

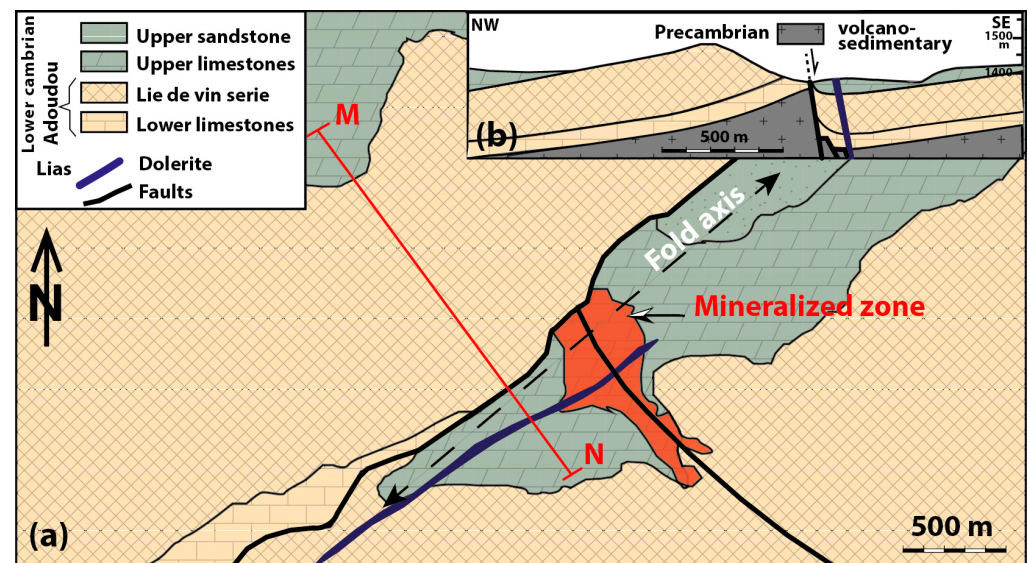


Figure 7. (a) Geological map of the Jbel Laassel mining district. (b) Geological cross-section M-N modified from Bourque et al. [21].

6. The Eastern Anti-Atlas Area and Associated Mineralization

South of Saghro where the Zagora-El Fecht ridge extends, only the lands of the Paleozoic cover outcrop. The Lower Cambrian is reduced to a few tens of meters in thickness. It is made up of sandstone and argillites intercalated with carbonate beds. The Middle Cambrian continues with the “Paradoxides Schists”. The Ordovician largely outcrops in the ridge; it is made up of a powerful silicoclastic series alternating between schist and sandstone formations [55,58]. The Silurian is essentially clayey with limestone at the top with *Orthoceras* [60]. The Devonian includes shales and limestones [26]. Numerous Lower Liassic doleritic dykes cut all of this area: Zagora and El Fecht. The deformation of this cover is attributed to Hercynian tightening [65].

6.1. Structural Data

In contrast to the western Anti-Atlas, post-Hercynian normal faults are common in the eastern Anti-Atlas [73]. On the Zagora-El Fecht Ridge, these faults are at the origin of two regional scale structures: the Zagora and the El Fecht grabens (Figure 8a). The first, most notable, extends over 70 km and is 1 to 5 km wide. At their eastern ends, the boundary faults branch into bundles, some of which cut through the overlying Maïder Paleozoic basin and continue beyond Taouz (south of Tafilalt), where they are overshadowed by the Cretaceous period [73]. At this eastern end, these faults form the Oumjrane-Taouz network faults, which control the mineralization of the Oumjrane-Bou n’Hass deposit [88] (Figure 8b). Hereafter, we describe in detail the Oumjrane-Bou n’Hass deposit and propose a genetic model for copper mineralization in the Paleozoic cover of the Zagora-El Fecht Ridge. To the west, the fault network is obscured by Quaternary alluvium but is recovered by Lower Ordovician subsidence along the long axis of the Bou Azzer inlier. From this location, it sailed to the WNW and joined the Anti-Atlas Major Fault of Choubert [89].

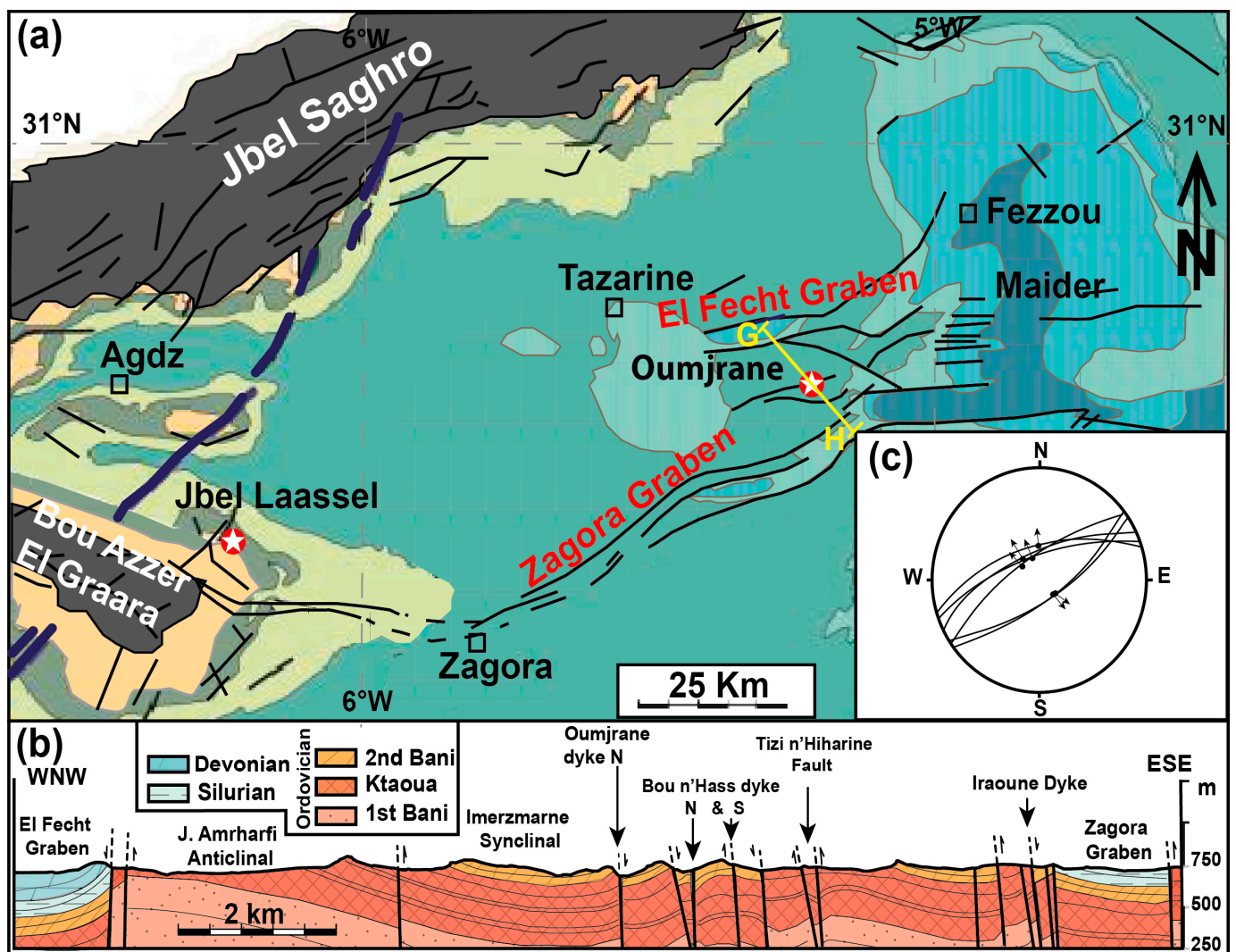


Figure 8. (a) Structural diagram showing the two major structures of the Zagora and El Fecht grabens (same legend as Figure 1), compiled from the geological maps of “Zagora-Elbow of the Drâa-Hamada of the Drâa” and “Todrha-Ma'der” at 1/200,000. (b) Geological cross-section (section G-H) of the Oumjrane-Bou n'Hass district (modified after Kharis et al. [90]). (c) Stereogram of normal fault planes (Schmidt canvas, lower hemisphere).

Along the main graben structures described above, the Silurian and Devonian units dip steeply, with a sudden change in inclination from horizontal to values greater than 45° , forming an asymmetrical syncline with adjacent flanks to the fault in upright positions. The direction of the fault oscillates between $N40^\circ$ and $N70^\circ$, with steep dips always greater than 60° . The geometric trial on fault surfaces presents a pitch between 75° and 90° . Stereographic projections of these structural data suggest a near-horizontal NW–SE extensional regime (Figure 8c). The principal stress axes are: $\sigma_3 = N150^\circ-75^\circ$ (minimum stress, extensional strain), $\sigma_2 = N60^\circ-20^\circ$ (intermediate stress), and $\sigma_1 = N150^\circ-0^\circ$ (maximum stress, compression). The same kinematics were deduced from the tectonic analyses of the Foug-Zguid area to within a few degrees. The resulting folds should have formed through passive bending in combination with lithostatic loading of the cover layers over the basement faults. The NW–SE faults commonly found in mineralized areas are coherent with such an extensional regime.

6.2. The Oumjrane-Bou n'Hass Deposit

Apart from some differences, the structure and event record of the Oumjrane-Bou n'Hass area are similar to the previous example. At this locality, the Paleozoic series was divided into many blocks by the N60° to N90° faults. The functioning of these normal faults induced the development of asymmetric folds of the N70° axis with straightened strata above major faults (Bou n'Hass and Oumjrane-Touaz faults). These local structures are superimposed on regional-scale axial NW–SE folds with long and short sides associated with basement strike-slip fault structures during Hercynian inversions [91–93].

The Oumjrane-Bou n'Hass site is characterized by the presence of collapsed structures represented by relatively large grabens (Zagora and El Fetch grabens). These extensional structures are clear evidence of a post-Hercynian extensional event. The mineralization here occurs in the form of near-vertical lenses of only a few tens of meters along the NE–SW to EW fault and the entire satellite fracture network (Figure 8b), but the peculiarity is that they follow each other along the same structural lineament. Their thickness can be locally small or even close to zero up to a few meters away. At the level of the walls, the filling contains angular sandstone fragments from nearby.

7. Mapping and the Morphological Interpretation of Deposits

Mapping the areas of deposits and mineralized occurrences provided two distinguished morphological deposits: stratiform and vein.

7.1. Stratiform Deposits

These are all located to the west of the Anti-Atlas and are spatially distributed along the NE–SW trend from the southern Ifni inlier to the Siroua massif (Figure 1). They are either in the Adoudou Formation, at the bottom of the “basal series” in contact with the Precambrian bedrock, or higher up in the Tamjout carbonate Formation, and rarely in the “Lower Limestones” Formation, but always in terrigenous facies with carbonate cement and/or in pure carbonate rocks. The main mineralized horizon, known as the Talat n'Ouamane horizon, is in the “Série de base” Formation between the top of its basal conglomerate and the Tamjout dolomite [7]. From bottom to top, it consists of coarse detrital levels with dolomitic cement, which grade to sandstone siltstone levels, followed by a series of dolomite formations topped with siltstone [7]. Within this horizon, mineralized zones form stratiform bodies that fill sedimentary joints and interlayered sliding surfaces. These bodies are thicker (tens of meters), closer together, have higher copper content, and exhibit significant lateral extension (over a kilometer) in those deposits where the hosted Adoudou Formation tends to lose strength such as in the Agjgal and Tazalaght deposits. Conversely, as the Adoudou Formation strengthens, the ore bodies depleted copper and thinned to disappear completely [7].

In stratiform bodies, mineralization occurred in different textural aspects (Figure 9): (i) filling voids of various sizes ranging from intragranular pores in carbonate-cemented terrigenous facies (Figure 9a) to those associated with open cavities in carbonate facies due to karstification and/or tectonic processes (Figure 9b), in the latter, undissolved carbonate residues are cemented by ore; (ii) in thin ribbons or veneers and coatings that develop along sedimentary fabrics and interlayered slipping planes parallel to the stratification planes (Figure 9c,d); (iii) in venules, sometimes branching into fine networks with no preferential orientation; (iv) in the dissemination of speckles of sulfides at first glance seemingly isolated, but interconnected by microcracks filled with calcite; (v) in granules lining internal geodes parallel to the bedding or directly connected to the veinlet network.

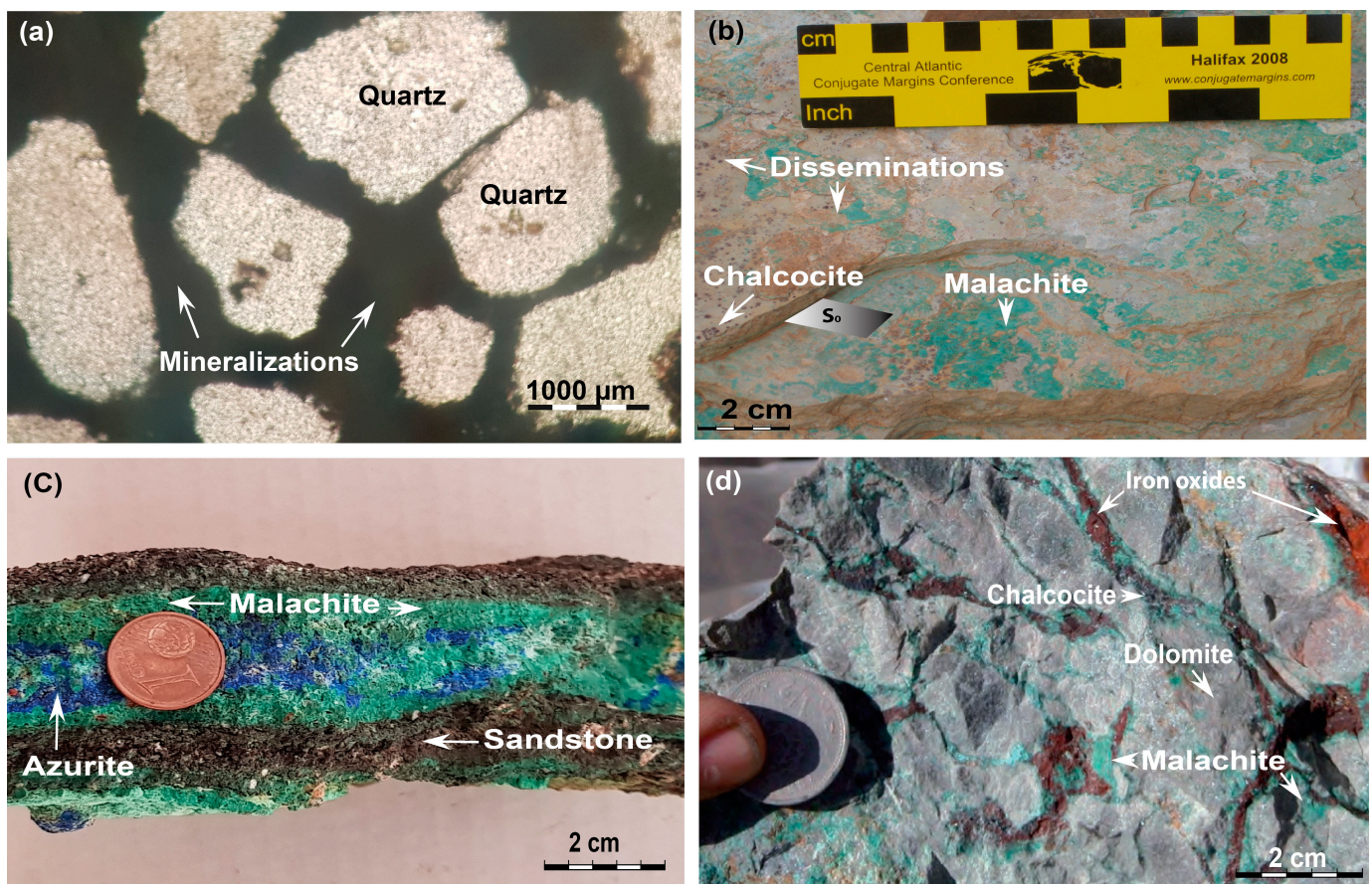


Figure 9. Main structure of the stratiform copper ores in the Anti-Atlas Paleozoic sedimentary. (a) Microscopic view of the cupriferous ore filling intragranular spaces of the sandstone facies of the “Série de base” Formation (Tazalaght deposit). (b) Structural karst-tectonic cavities in dolomite filled with oxidized chalcocite to malachite and iron oxides (Agjgal deposit, Maddy et al. [14]). (c) bands of malachite and azurite conformable to bedding (Tazalaght deposit). (d) Malachite veneers and chalcocite grains lining the Adoudounian limestone stratification planes north of Tayfast (Central Anti-Atlas).

7.2. Vein Deposits

In the central and eastern part of Anti-Atlas, copper deposits consist of veins developed along the NNW–SSE to NS sub-vertical fracture in the Jbel Laassel and Timarighine deposits and NE–SW to E–W fractures in the Oumjrane-Bou n’Hass deposit (Figure 10a). Their horizontal extent is sometimes more than a kilometer, but in most cases, they are small lenticular bodies. These ore bodies can narrow up or thicken to several meters along the same fault. The same vein morphological changes (bulges and retracted) as on the plane were also observed in the working face sections (Figure 10b), indicating that the mineralization is distributed in the columns. The filling of the first band is repeatedly reworked to breccia in the second band, suggesting that fracture reactivations control mineralization. Along the same fault, veins sometimes branch into thin veinlets that become highly entangled (stockworks) and form economically mineable bodies such as the Jbel Laassel deposit (Figure 10c).

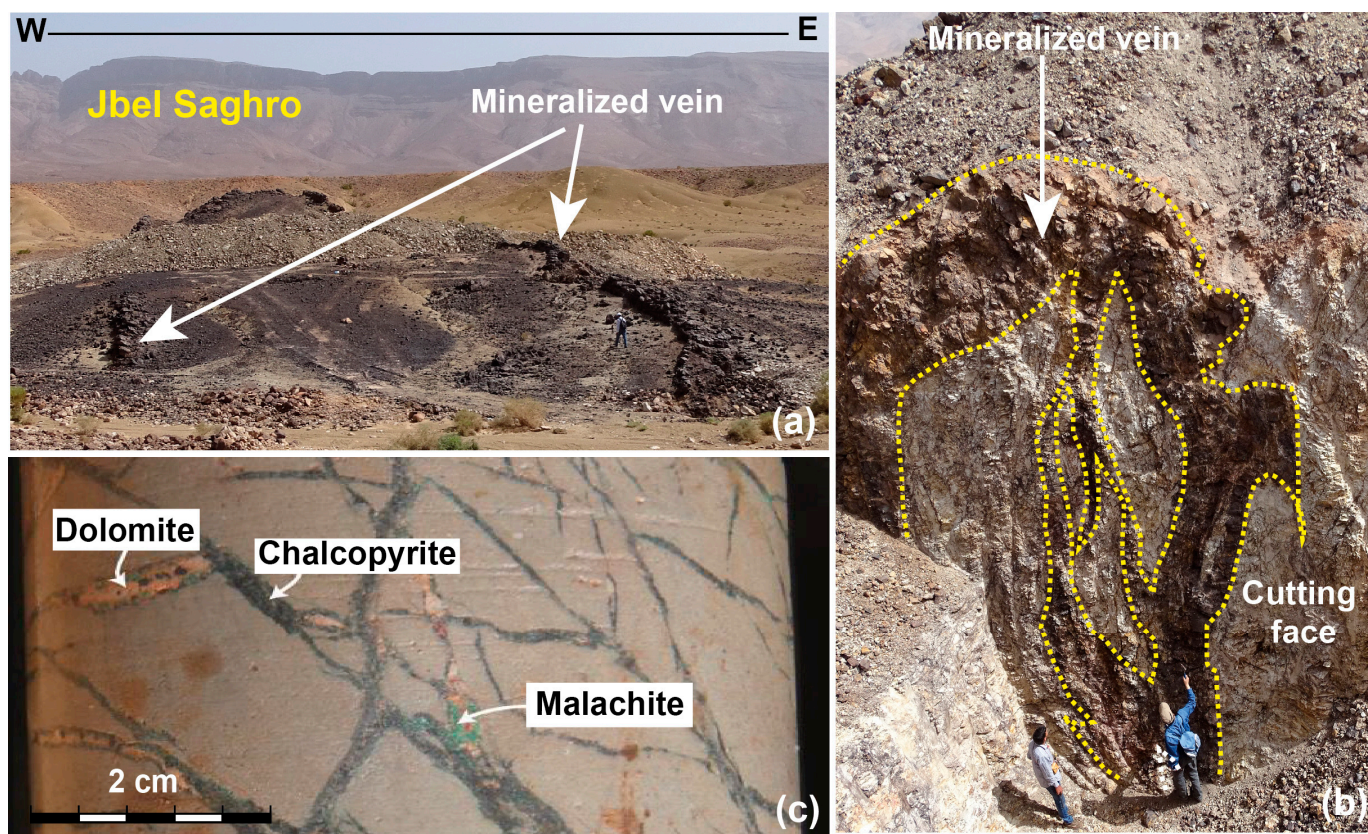


Figure 10. (a) Mineralized veins of Timarighine, south of Saghro (N 30°52′39, 33″; W 5°36′49, 83″). (b) Sectional view illustrating the morphological variations (thickening, thinning, branching) of the veins. (c) Chalcocite, malachite, and dolomite stockwork (core sample from Jbel Laassel, Bourque [21]).

7.3. General Deduction

The main Anti-Atlas copper deposits are located in the west and are usually stratiform in appearance. Outside the “Série de base” of the Adoudou Formation, mineralization becomes vein-type. These morphological features lead to the treatment of stratiform mineralization as the syngenetic variant and vein pattern as the epigenetic variant. It should be noted, however, that this seemingly logical explanation does not take into account the spatiotemporal distribution of mineralization, nor the tectonomagmatic phenomena that accompany it. Therefore, these unique morphological features alone cannot be used to discriminate genetic processes. An acceptable interpretation requires additional criteria.

7.4. The Lateral Distribution and Morphological Effects of Mineralization

The spatial distribution model for this copper mineralization case is based on a regional mapping approach. It includes a compilation of available data for the major copper deposits in the Anti-Atlas [7,21,23,90,93–99]. This approach revealed significant differences in deposit density and its lateral distribution, manifested by the presence of three corridors with the most pronounced concentrations of mineralization (Figure 1). These corridors qualified as rich ridges by Bouchta et al. [94], narrow southwest–northeast corridors oriented obliquely on the ENE–WSW direction of the Anti-Atlas. One of their particularities is that they are all longitudinally bisected by normal fault and traversed by CAMP doleritic dykes (Igherm dyke, Foum-Zguid dyke, and Zagora El Fetch dyke), from which these rich corridors are named. Therefore, we can distinguish the western ridge of Igherm, the central ridge of Foum-Zguid, and the eastern ridge of Zagora-El Fecht (Figure 1). These tectonomagmatic corridors appear to control copper deposits within the Lower Paleozoic cover and must have influenced the genetic process of the mineralization. The association

of these extensive tectonic structures with CAMP magmatism implicitly suggests that the copper hosted in the Lower Paleozoic cover of the Anti-Atlas is post-Hercynian. In the vision we defend in this note, crustal extension occurring concurrently with the Central Atlantic opening would provide a favorable geodynamic and thermal environment for the reconcentrations of copper mineralization. Nevertheless, this new hypothesis must be supported by other arguments before it can be tested.

7.5. Stratigraphic Distribution and Genetic Significance

Mapping of major copper concentrations and mineable deposits also shows that the Paleozoic sedimentary layers hosting the mineralization vary by region. Mineralization is indeed abundant along the western ridge of Igherm (Tazalaght, Aggal, etc.), and is hosted by the “Série de base” Formation and/or by the Tamjout dolomite. In the Central Anti-Atlas area, mineralization is located higher in the Upper Limestone Formation at Jbel Laassel [21] and more in the 2nd Bani Group sandstones of the Ordovician to the east (Oumjrane-Bou n’Hass) [84]. This distribution is not arbitrary, since in all cases, it emphasizes that copper is deposited in the lower levels, not far from the basement–cover interface. The Lower Cambrian transgression coming from the west of the Anti-Atlas started with the “Séries de base” Formation, which was restricted to the bay of the western Igherm ridge. To the east, the entire Adoudou Formation disappears at the level of the central Anti-Atlas, and further east, the Middle Cambrian and Ordovician sandstones occupy a relatively basal position, directly overlaying the Precambrian basement. If the location of copper mineralization is indeed independent of the stratigraphic level of the sedimentary cover, certainly, its occurrence always highlights the Proterozoic–Paleozoic transition and thus the contact between the rigid basement and the sedimentary cover. It is most likely that the lithological characteristics of the transition from a brittle basement to a flexible cover would have facilitated the establishment of mineralization.

7.6. Features and Differences

Within the Igherm and Fom-Zguid Ridges, iron oxides are closely related to copper, and sometimes, the iron/copper ratio can reach only iron poles, especially around the Agadir Melloul, Taifast, Iguerda, and Zenaga areas, where many oligist quartz veins are artisanal mines [100]. In the Zagora-El Fecht Ridge, mineral occurrences are dominated by Ba, which is related to Pb and Zn, forming zonality away from the copper mining area.

In addition to these mineralogical differences, there are tectonic structures that are not uniform at the Anti-Atlas scale. Moreover, these large eastward dipping faults are becoming more common in the central and eastern Anti-Atlas [73]. These extensional structures, especially in the eastern Anti-Atlas region, are easy to spot in the landscape when they affect very high-contrast formations. Their vertical offset is weak (Figure 11a,b), rarely exceeding ten meters, as they are usually only observed on annexed small faults with weak displacements rather than large ones. In the western Anti-Atlas region, the post-Hercynian normal faults are rarely observed (Figure 11c), but a series of Mesozoic–Cenozoic burials and exhumations have been demonstrated in the Anti-Atlas by thermochronological methods and are attributed to the post-Hercynian movements [101–104].

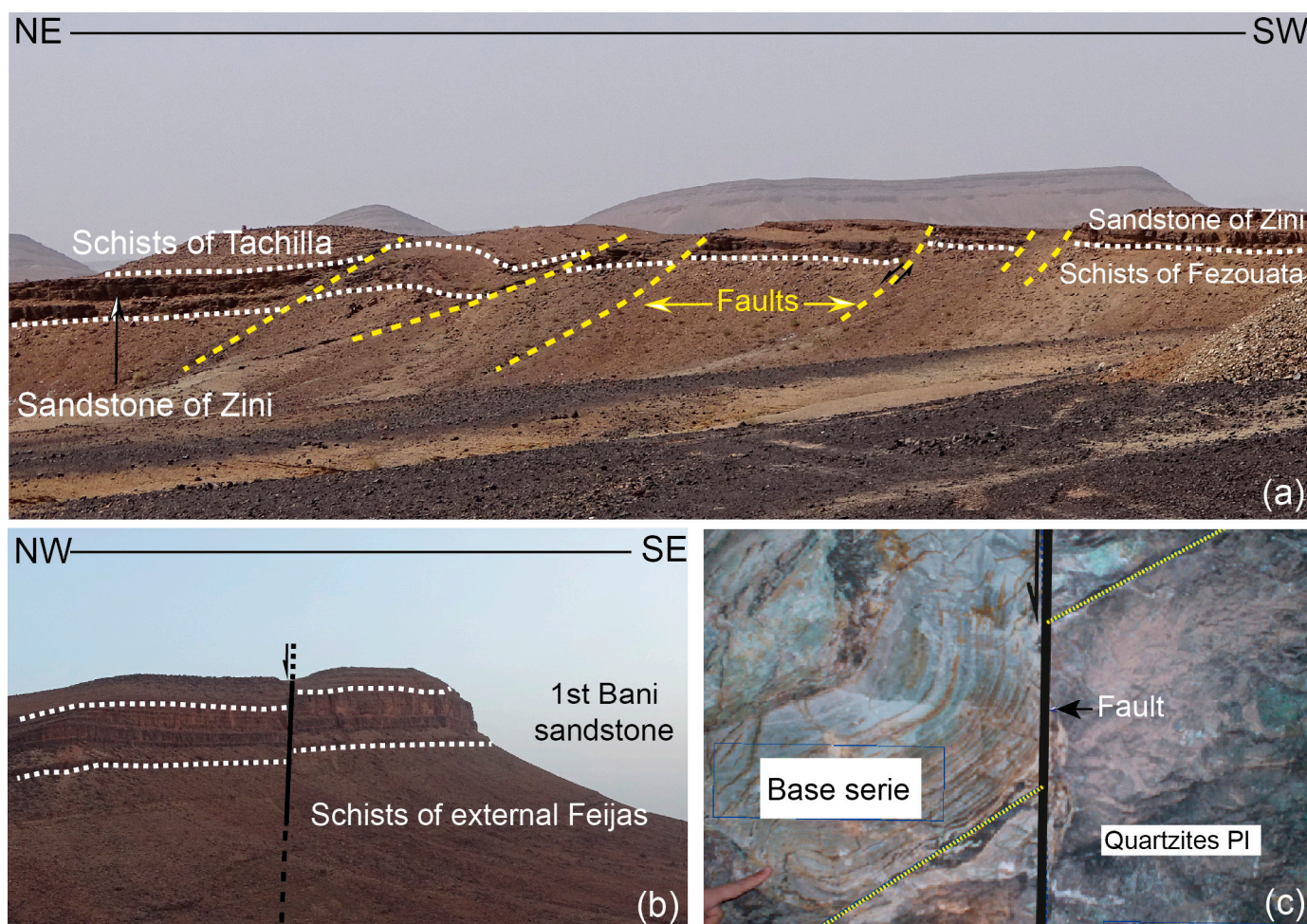


Figure 11. (a) Network of normal faults offsetting the Ordovician terrains and hosting the copper veins of Timarighine (Eastern Anti-Atlas). (b) Normal fault shifting the sandstone bar of the 1stBani to the west of Tazarine (eastern Anti-Atlas). (c) Subsidence of the “Série de base” Formation along a normal fault affecting the Paleoproterozoic (PI) basement in a gallery at the Tazalaght mine (after Tahir et al. [105]).

8. Mineralogy

The common feature of these two morphological types of mineralization is that they all present a simple mineral association consisting of a hypogene paragenesis with bornite, chalcopyrite, and incidentally pyrite and a supergene paragenesis with copper-enriched mineral phases; native copper, chalcocite, covellite, malachite, and azurite (Figure 12). Pb (galena) and Zn (blende) sulfides are rare or even absent, except in the Bou Skour deposit and a few localized showings in the Tamjout Formation. These sulfides should in no way be confused with galena and sphalerite (blende) encountered in the occurrences that form a lead-zinciferous belt all around the Anti-Atlas copper domain: Jbel Jaouad and Bou Lbaroud deposits to the west, the Addana veins to the south, and the deposits of Ougnat and the Tafilalt region to the east [24] (Figure 1).

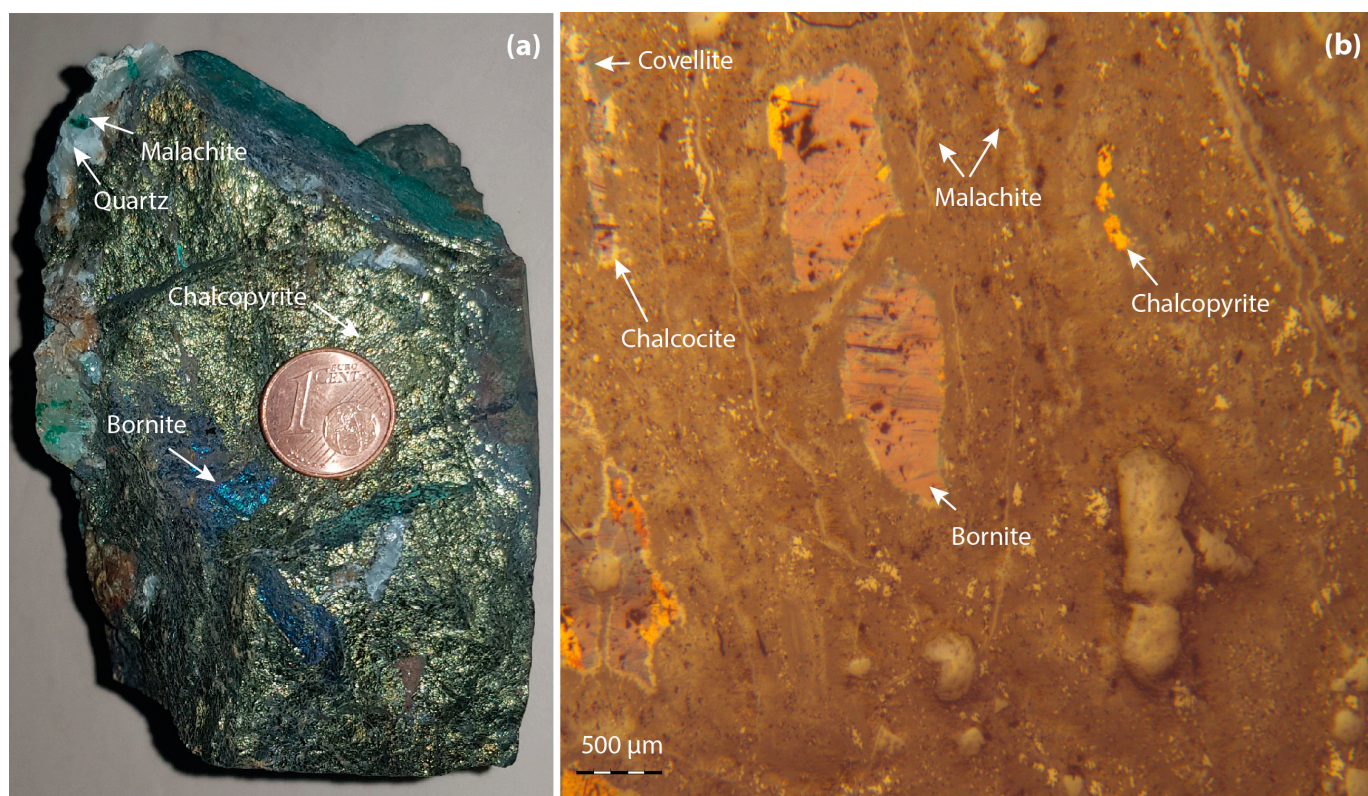


Figure 12. (a) Main mineral phases of the ore. (b) Microscopic appearance in the reflected light of the polished section of the primary paragenesis with chalcopyrite (yellow) and bornite (brown-purple) in the process of being transformed into chalcocite (grey-white), covellite (blue), and malachite (light grey), all bathed in a range of iron oxides and hydroxides.

9. Discussion and Genetic Model

The large numbers of copper deposits in the Anti-Atlas Lower Paleozoic series are closely concentrated in fold structures generated directly on basement extensional faults. These are large folds flanked by one or more normal faults on one side. They intersect the entire Paleozoic stratigraphic column in the eastern Anti-Atlas but vanish long before reaching the surface in the western Anti-Atlas. Throughout the Anti-Atlas, these folded structures systematically remodel the Hercynian folds axis, attesting to their post-Hercynian occurrence, as is the case at Jbel Laassel [21].

Copper mineralization, especially vein-style copper deposits, fills the faults, fissures, and veins that develop on the outer hinge of the faulted folds. Therefore, this mineralization occurred concurrently with the folding process, which may have been driven by extensive faulting, if not later. In addition to the post-Hercynian folds and faults, the doleritic dykes in the same orientation traverse the corridor of concentrated mineralization, and these elements are sufficient to form a complete mineralization system. Dykes provide the necessary heat to remobilize mineralized fluids, while open faults in rigid bedrock serve as drains toward traps typically developed at the level of folded sedimentary cover above basement faults. These stratigraphic, tectonic, and magmatic arguments point to a broad post-Hercynian geodynamic setting that can correspond to the Late Triassic–Liassic rifting. In fact, in the Tafilalt area, the oldest post-folding sediments are Triassic [73], confirming Boissavy's [91] already old observation in the Maïder area, where the youngest deformed terrain was Stephanian and Cretaceous transgressive deposits on the Paleozoic was unfolded. This extended magmatic manifestation resulted in the emplacement of a network of mafic dykes attributed to the CAMP [104] following the old NE–SW fault.

In detail, this crustal stretching caused the reactivation of basement fractures beneath the flexible sedimentary cover. The NE–SW faults are remobilized as normal faults and the NNW–

SSE faults as strike-slip faults. The vertical motion of the NE–SW accident resulted in the formation of asymmetric folds with a near-horizontal axis, characterized by a steep limb and the other limb slightly sloping toward the heart of the structure. This type of fold is common in extensional systems [105]. Khalil and McClay [106] described similar folds in the Duwi and Hamadat belts on the northwestern margin of the Red Sea Rift System, where a similar evolution can be traced. They are also described in experimental models [107–109]. In the south of Tafilalt, Robert-Charrue and Burkhard [75] described similar folds in Devonian and Carboniferous strata and attributed them to the post-Hercynian extensional event. According to the same authors, these structures associated with normal faults are even more puzzling because they present slip movements between layers of planes, leading to confusion with Hercynian folds. Equally perplexing is the coexistence of normal and reverse faults in this type of fold, as is well-demonstrated in the Rattlesnake Mountain Anticline (Wyoming, USA) [84].

The basement faults that produced these folds do not always cut the entire Paleozoic series like in the Issafène fold structure because of its inhomogeneous rheology. This mechanism is well-illustrated by the extensional Trishear model [110]. According to the model, fixed marks separated from fault by plastic layers, “clays, siltstones”, form drag folds that dampen the propagation of these faults toward the top of the sedimentary pile.

Deformation is accommodated in these folded structures through multiple fractures (joints, tension gashes, faults, and block lodes) and sliding along specific fracture planes. These and the entire pore system from intragranular pores of terrigenous carbonate-cemented facies to pores in pure carbonate facies opened by the karstification experienced during Carboniferous exhumation act as mineralized traps. In addition, NNW–SSE faults usually reactivate on slip faults where the mineralization field relays open areas compatible with a transtensional regime. Mineralization also occurs in the form of en échelon lenses along the NE–SW faults.

The various textures exhibited by the ore—veins, veinlets, stockwork, dissemination, filling of karst voids, thin bands between sedimentary layers, or slip planes between bedding—appear to be the source of the controversies surrounding the mechanisms of copper supply and precipitation formulated in previous works.

The occurrence of copper mineralization in the Anti-Atlas Lower Paleozoic cover was governed by the CAMP tectonomagmatic event, associated with the Upper Triassic fragmentation of Pangea. At that time, the Anti-Atlas is considered to be the southern shoulder of the northern Atlas-Triassic rift and can be viewed as a large area undergoing a left-lateral transtensional tectonic regime, bordered northward by the South Atlas Fault [111–114] and by the Bas Drâa Fault at the foot of Jbel Ouarkziz to the south [25]. Between these two regional lineaments is a stretched area that develops en échelon fault corridors filled with CAMP doleritic magma (Figure 13). The magmatic emplacement guided by the NE–SW faults warmed the continental crust. The associated heat flow gives rise to convective cells that drain hydrothermal fluids from deep along inherited tectonic accidents. They mobilize copper through a crystalline basement that does not preclude the remobilization of pre-existing mineralization, and then they migrate upward to settle in a series of fractures and voids developed within passive folds developed above NE–SW normal faults (Figure 14). The paleoreliefs spatially associated with copper mineralization [14,63] have not been questioned insofar as they could be assimilated to preferential zones of basement high delimited by normal faults.

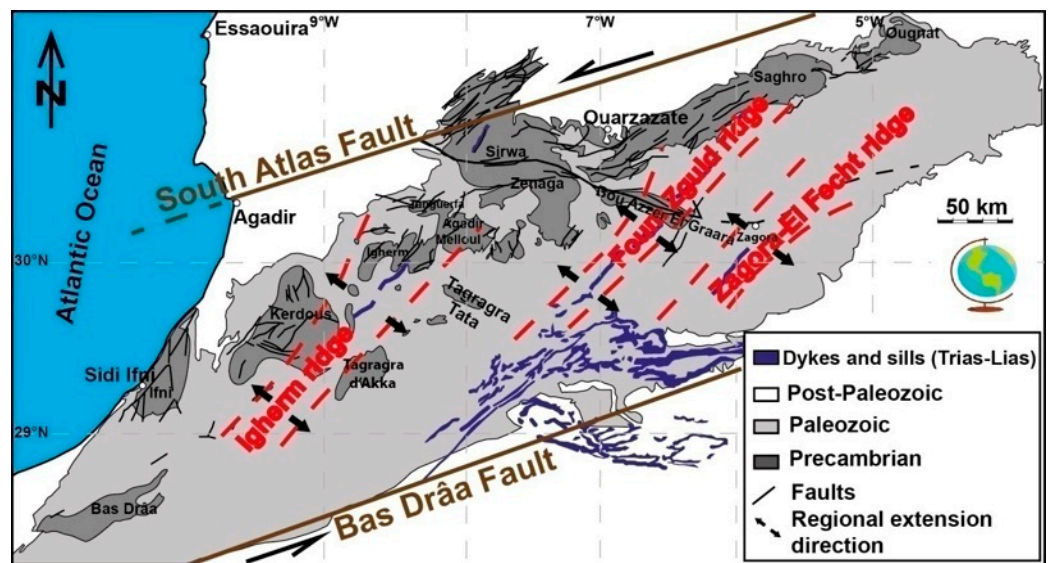


Figure 13. Interpretative structural map of the Anti-Atlas during the Late Triassic–Lower Liassic.

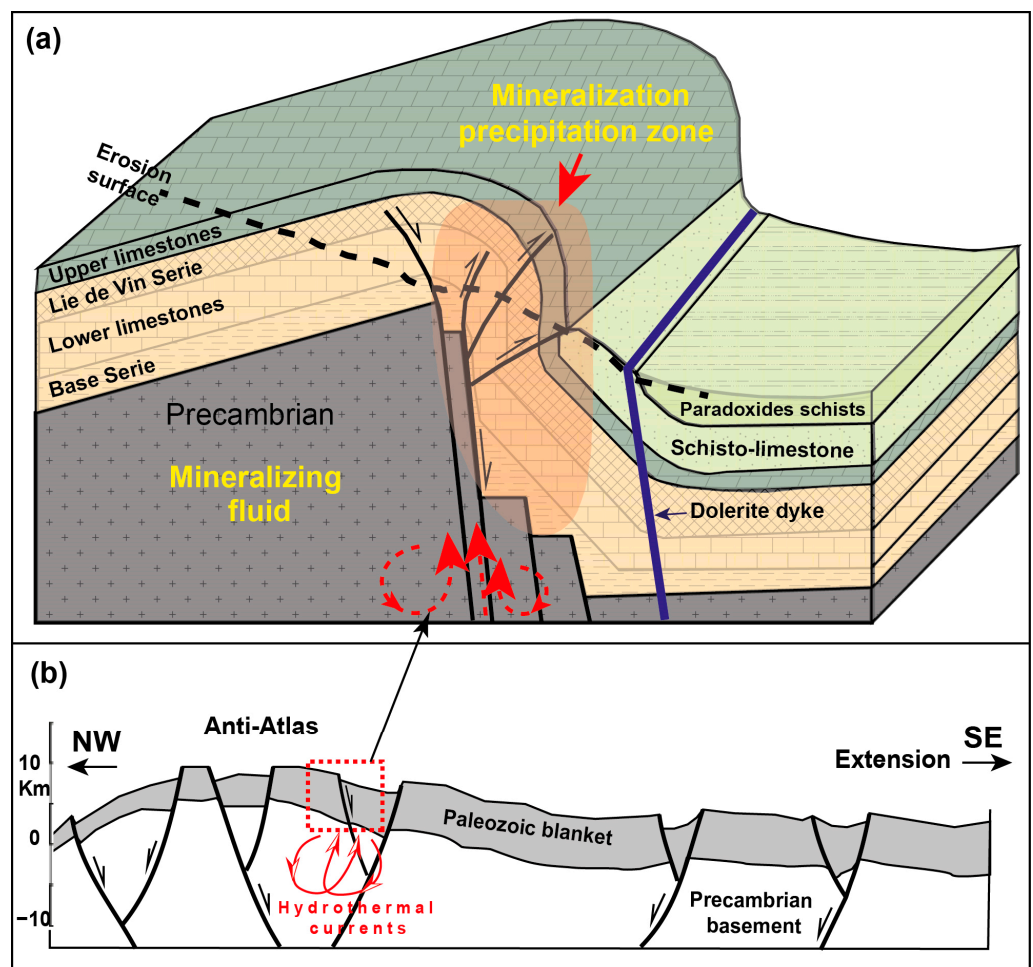


Figure 14. (a) Model illustrating the occurrence of copper mineralization in the Paleozoic cover of the Anti-Atlas. (b) Schematic NNW–SSE geological section of the Anti-Atlas during the Triassic–Liassic extension (reactivation of deep fractures and creation in the cover of steep normal faults and associated folds).

10. Conclusions

The Anti-Atlas hosts numerous copper-dominated deposits and occurrences, conferring its status as a copper province [24,94]. The report on the map of the location of these metalliferous deposits shows significant differences in their distribution density, revealing the three most notable areas of concentration. These narrow and SW–NE-oriented areas are crossed longitudinally by normal faults and doleritic dykes associated with the Late Triassic–early Liassic Central Atlantic opening. Faults do not always affect the entire Paleozoic cover; their presence in outcrops manifests as noticeable flexures under which passive folds develop with a series of cracks and openings. All of these discontinuities and voids contribute to the circulation and deposition of copper mineralization, resulting in diverse textural aspects of the ore: veins, veinlets, stockwork, dissemination, filling of karstic voids, thin ribbons between sedimentary fabrics or following the inter-bed sliding planes parallel to the stratigraphic binding, and intragranular pores in the terrigenous facies with carbonate cement. This fact appears to be the source of the controversies raised in previous works on copper contribution and precipitation mechanisms.

However, the origin of copper metal remains unclear. We have seen from above that the best-documented source of copper is the Upper Ediacaran magmatism of the Ouarzazate Group, not excluding remobilized parts from the earlier basement. Given that most Triassic basins preserved in the High Atlas have not been associated with significant mineralization, the possible contribution of the CAMP event has not been confirmed, although other deposits such as fluorite at the El Hammam mine in the Moroccan Meseta have been documented as associated with the CAMP event.

In any case, the precipitation of the ore is controlled by changes in the physicochemical conditions of the liquid, especially the temperature drop. Such models integrate all morphological data, but most importantly textural data, which at first glance seems incoherent and give rise to controversial interpretations.

Author Contributions: Conceptualization, M.O., E.H.A., and A.S.; Methodology, E.H.A., A.S., and B.L.; Software, E.H.A. and M.A.; Validation, M.O., B.L., M.B., K.A., T.A.-A., F.Z.E., and S.B.; Formal analysis, E.H.A. and A.S.; Investigation, E.H.A.; Resources, M.O. and E.H.A.; Data curation, M.O. and E.H.A.; Writing—original draft preparation, M.O., E.H.A., A.S., and M.B.; Writing—review and editing, M.A., B.L., K.A., T.A.-A., and S.B.; Visualization, M.O., M.A., and F.Z.E.; Supervision, E.H.A.; Project administration, M.A.; Funding acquisition, K.A. All authors have read and agreed to the published version of the manuscript.

Funding: This research was funded by the Researchers Supporting Project number RSP2023R351, King Saud University, Riyadh, Saudi Arabia.

Data Availability Statement: Not applicable.

Conflicts of Interest: The authors declare no conflict of interest.

References

1. Rosenberger, B. Les vieilles exploitations minières et les anciens centres métallurgiques du Maroc, essai de carte historique-1. *Rev. Géogr. Maroc.* **1970**, *17*, 71–108.
2. Rosenberger, B. Les vieilles exploitations minières et les anciens centres métallurgiques du Maroc, essai de carte historique-2. *Rev. Géogr. Maroc.* **1970**, *18*, 59–102.
3. Saadi, M. Les gisements de cuivre de Bleïda (Graara, Anti-Atlas, Maroc). In *Les Roches Plutoniques dans leurs Rapports avec les Gîtes Minéraux*; Masson: Paris, France, 1973; pp. 288–290.
4. Leblanc, M.; Billaud, P.A. Volcano-sedimentary copper deposit on a continental margin of upper Proterozoic age; Bleida (Anti-Atlas, Morocco). *Econ. Geol.* **1978**, *73*, 1101–1111. [[CrossRef](#)]
5. Mouttaqi, A.; Sagon, J.P. Le gisement de cuivre de Bleida (Anti-Atlas central): Une interférence entre les processus de remplacement et d'exhalaison dans un contexte de rift. *Chron. Rech. Min.* **1999**, *536–537*, 5–21.
6. Maacha, L.; Ennaciri, O.; El Ghorfi, M.; Baoutoul, H.; Saquaque, A.; Soulaïmani, A. Le cuivre oxydé du J. La'sal (boutonnière d'El Graara, Anti-Atlas central). In *Nouveaux Guides Géologiques et Minières du Maroc, Les Principales Mines du Maroc*; Mouttaqi, A., Rjmati, E.C., Maacha, L., Michard, A., Soulaïmani, A., Ibouh, H., Eds.; Notes et Mémoires du Service Géologique du Maroc; Ministère de l'Énergie, des Mines, de l'Eau et l'Environnement: Rabat, Morocco, 2011; Volume 9, pp. 117–121.

7. Pouit, G. Paléogéographie et répartition des minéralisations stratiformes de cuivre dans l'Anti-Atlas occidental (Maroc). *Chron. Rech. Min.* **1966**, *34*, 279–289.
8. Chabane, A.; Boyer, C. Séries volcaniques et minéralisations cuprifère du Précambrien supérieur de Tanguerfa, Anti-Atlas, Maroc. *C. R. Acad. Sci. Paris* **1979**, *288*, 5–8.
9. Boyer, C.; Boyer, F. Les minéralisations cuprifères liées au volcanisme calco-alcalin de l'Anti-Atlas du Maroc (précambrien terminal). Comparaison avec les gisements de type "Mantos" des Andes. *Chron. Mines Rech. Min.* **1982**, *468*, 5–30.
10. Leblanc, M. Appareil ignimbrétique et minéralisation cuprifère: Alous (Anti-Atlas, Maroc). *Mineral. Depos.* **1986**, *21*, 129–136. [[CrossRef](#)]
11. Chebbaa, B. Métallogénie du Cuivre Associé aux Roches Volcaniques d'âge Précambrien III Supérieur dans l'Anti-Atlas Marocain. Ph.D. Thesis, Lausanne University, Lausanne, Switzerland, 1996.
12. Skacel, J. Gisement cuprifère polygénétique de Tazalaght (Anti-Atlas occidental). *Mines Géol. Energ.* **1993**, *54*, 127–133.
13. Benssaou, M.; Hamoumi, N. Paléoenvironnements et minéralisations de l'Anti-Atlas occidental marocain au Cambrien précoce. *Chron. Mines Rech. Min.* **1999**, *536–537*, 113–119.
14. Maddi, O.; Baoutoul, H.; Maacha, L.; Ennaciri, O.; Soulaïmani, A. La mine d'Agjgal au sud du Kerdous; considérations sur les gîtes stratoïdes de cuivre et argent de l'Anti-Atlas occidental et central. In *Nouveaux Guides Géologiques et Miniers du Maroc, Principales Mines du Maroc*; Mouttaqi, A., Rjimati, E.C., Maacha, L., Michard, A., Soulaïmani, A., Ibouh, H., Eds.; Notes et Mémoires du Service Géologique du Maroc; Ministère de l'Énergie, des Mines, de l'Eau et l'Environnement: Rabat, Morocco, 2011; Volume 9, pp. 151–156.
15. Oummouch, A.; Essaifi, A.; Zayane, R.; Maddi, O.; Zouhair, M.; Maacha, L. Geology and metallogenesis of the sediment-hosted Cu-Ag deposit of Tizert (Igherm inlier, Anti-Atlas Copperbelt, Morocco). *Geofluids* **2017**, *2017*, 7508484. [[CrossRef](#)]
16. Benssaou, M.; M'Barki, L.; Ezaidi, A.; Abioui, M. Geodynamic Significance of Stacking Lower Cambrian Sequences Units in the Western Anti-Atlas. *Int. J. Mater. Sci. Appl.* **2017**, *6*, 142–147. [[CrossRef](#)]
17. Fauvelet, E. *Réflexions sur une liaison possible entre les Minéralisations cuprifères et les roches plutoniques basiques hercyniennes dans l'Anti Atlas (Maroc)*; Masson: Paris, France, 1973.
18. Clavel, M.; Leblanc, M. Liaison entre tectonique et minéralisation cuprifère dans les dolomies infracambriennes de la région du Jbel N'Zourk (Anti-Atlas central, Maroc). *Notes Serv. Géol. Maroc.* **1971**, *237*, 229–232.
19. Anthonioz, P.M.; Bahi, L.; Khalek, M. Karstic metalliferous concentration in a discontinuous carbonated environment-cupriferous deposit of Amadouze (Western Anti-Atlas, Morocco). *C. R. Acad. Sci.* **1979**, *288*, 1251–1253.
20. El Basbas, A. Caractérisation Métallogénique de la Minéralisation Cuprifère de l'Anti-Atlas Occidental (Maroc): Cas des Gisements de Tazalaght, Agoujgal et Ouansimi. Ph.D. Thesis, Moulay Ismail University, Meknès, Morocco, 2015.
21. Bourque, H.; Barbanson, L.; Sizaret, S.; Branquet, Y.; Ramboz, C.; Ennaciri, A.; El Ghorfi, M.; Badra, L. A contribution to the synsedimentary versus epigenetic origin of the Cu mineralizations hosted by terminal Neoproterozoic to Cambrian formations of the Bou Azzer–El Graara inlier: New insights from the Jbel Laassel deposit (Anti Atlas, Morocco). *J. Afr. Earth Sci.* **2015**, *107*, 108–118. [[CrossRef](#)]
22. Smeykal, S. Traits géologiques du gisement cuprifère d'Ouansimi. Anti-Atlas occidental. *Mines Géol.* **1972**, *35*, 21–34.
23. Soulaïmani, A.; Le Corre, C.; Farazdaq, R. Déformation hercynienne et relation socle/couverture dans le domaine du Bas-Drâa (Anti-Atlas occidental, Maroc). *J. Afr. Earth Sci.* **1997**, *24*, 271–284. [[CrossRef](#)]
24. Routhier, P. Où sont les métaux pour l'avenir? Les provinces métalliques. Essai de métallogénie globale. *Mém. BRGM* **1980**, *105*, 410p.
25. Choubert, G. Histoire géologique du domaine de l'Anti-Atlas. *Notes Mém. Serv. Géol. Maroc.* **1952**, *6*, 77–172.
26. Abia, E.H.; Benssaou, M.; Abioui, M.; Ettayfi, N.; Lhamyani, B.; Boutaleb, S.; Maynard, J.B. The Ordovician iron ore of the Anti-Atlas, Morocco: Environment and dynamics of depositional process. *Ore Geol. Rev.* **2020**, *120*, 103447. [[CrossRef](#)]
27. Cox, D.P.; Singer, D.A. (Eds.) *Mineral Deposit Models*; US Geological Survey: Lawrence, KA, USA, 1992.
28. Jébrak, M.; Marcoux, E. *Geology of Mineral Resources; Geology of Quebec*: Quebec, QC, Canada, 2008; 667p.
29. Mouttaqi, A.; Rjimati, E.C.; Maacha, L.; Michard, A.; Soulaïmani, A.; Ibouh, H. *Les Principales Mines du Maroc*; Notes et Mémoires du Service Géologique du Maroc; Ministère de l'Énergie, des Mines, de l'Eau et l'Environnement: Rabat, Morocco, 2011; Volume 9, 374p.
30. Choubert, G. Histoire géologique du précambrien de l'Anti-Atlas. *Notes Mém. Serv. Géol. Maroc.* **1963**, *162*, 352p.
31. Soulaïmani, A.; Burkhard, M. The Anti-Atlas chain (Morocco): The southern margin of the Variscan belt along the edge of the West African Craton. *Geol. Soc. Lond. Spec. Publ.* **2008**, *297*, 433–452. [[CrossRef](#)]
32. Clauer, N. Géochimie Isotopique du Strontium des Milieux sédimentaires. Application à la Géochronologie de la Couverture du Craton Ouest-Africain. Ph.D. Thesis, University of Strasbourg, Strasbourg, France, 1976.
33. Leblanc, M.; Lancelot, J. Interprétation géodynamique du domaine panafricain de l'Anti-Atlas (Maroc) à partir de données géologiques et géochronologiques. *Can. J. Earth Sci.* **1980**, *17*, 142–155. [[CrossRef](#)]
34. Thomas, R.J.; Chevallier, L.P.; Gresse, P.G.; Harmer, R.E.; Eglinton, B.M.; Armstrong, R.A.; De Beer, C.H.; Martini, J.E.J.; De Kock, G.S.; Macey, P.H. Precambrian evolution of the Sirwa window, Anti-Atlas orogen, Morocco. *Precambrian Res.* **2002**, *118*, 1–57. [[CrossRef](#)]
35. Kouyaté, D.; Söderlund, U.; Youbi, N.; Ernst, R.; Hafid, A.; Ikenne, M.; Soulaïmani, A.; Bertrand, H.; Chaham, K.R. U–Pb baddeleyite and zircon ages of 2040 Ma, 1650 Ma and 885 Ma on dolerites in the West African Craton (Anti-Atlas inliers): Possible links to break-up of Precambrian supercontinents. *Lithos* **2013**, *174*, 71–84. [[CrossRef](#)]

36. El Bahat, A.; Ikenne, M.; Söderlund, U.; Cousens, B.; Youbi, N.; Ernst, R.; Soulaïmani, A.; Hafid, A. U–Pb baddeleyite ages and geochemistry of dolerite dykes in the Bas Drâa Inlier of the Anti-Atlas of Morocco: Newly identified 1380 Ma event in the West African Craton. *Lithos* **2013**, *174*, 85–98. [[CrossRef](#)]
37. Youbi, N.; Kouyaté, D.; Söderlund, U.; Ernst, R.E.; Soulaïmani, A.; Hafid, A.; Ikenne, M.; El Bahat, A.; Bertrand, H.; Chaham, K.R. The 1750 Ma magmatic event of the west African craton (Anti-Atlas, Morocco). *Precambrian Res.* **2013**, *236*, 106–123. [[CrossRef](#)]
38. Saquaque, A.; Admou, H.; Karson, J.; Hefferan, K.; Reuber, I. Precambrian accretionary tectonics in the Bou Azzer-El Graara region, Anti-Atlas, Morocco. *Geology* **1989**, *17*, 1107–1110. [[CrossRef](#)]
39. Blein, O.; Baudin, T.; Soulaïmani, A.; Cocherie, A.; Chèvremont, P.; Admou, H.; Ouanaïmi, H.; Hafid, A.; Razin, P.; Bouabdelli, M. New geochemical, geochronological and structural constraints on the Ediacaran evolution of the south Sirwa, Agadir-Melloul and Iguerda inliers, Anti-Atlas, Morocco. *J. Afr. Earth Sci.* **2014**, *98*, 47–71. [[CrossRef](#)]
40. Soulaïmani, A.; Ouanaïmi, H.; Saddiqi, O.; Baidder, L.; Michard, A. The Anti-Atlas Pan-African Belt (Morocco): Overview and pending questions. *C. R. Géosci.* **2018**, *350*, 279–288. [[CrossRef](#)]
41. Inglis, J.D.; D’Lemos, R.S.; Samson, S.D.; Admou, H. Geochronological constraints on Late Precambrian intrusion, metamorphism, and tectonism in the Anti-Atlas Mountains. *J. Geol.* **2005**, *113*, 439–450. [[CrossRef](#)]
42. Choubert, G.; Hupé, P. Le Précambrien III et le Géorgien de l’Anti-Atlas. *Notes Mém. Serv. Géol. Maroc.* **1953**, *103*, 7–39.
43. Michard, A.; Soulaïmani, A.; Hoepffner, C.; Ouanaïmi, H.; Baidder, L.; Rjimati, E.C.; Saddiqi, O. The south-western branch of the Variscan Belt: Evidence from Morocco. *Tectonophysics* **2010**, *492*, 1–24. [[CrossRef](#)]
44. Soulaïmani, A.; Bouabdelli, M.; Piqué, A. The Upper Neoproterozoic–Lower Cambrian continental extension in the Anti-Atlas (Morocco). *Bull. Soc. Géol. Fr.* **2003**, *174*, 83–92. [[CrossRef](#)]
45. Benssaou, M.; Hamoumi, N. The western Anti-Atlas of Morocco: Sedimentological and palaeogeographical formation studies in the Early Cambrian. *J. Afr. Earth Sci.* **2001**, *32*, 351–372. [[CrossRef](#)]
46. Benssaou, M.; Hamoumi, N. Le graben de l’Anti-Atlas occidental (Maroc): Contrôle tectonique de la paléogéographie et des séquences au Cambrien inférieur. *C. R. Géosci.* **2003**, *335*, 297–305. [[CrossRef](#)]
47. Geyer, G. The base of a revised Middle Cambrian: Are suitable concepts for a series boundary in reach? *Geosci. J.* **2005**, *9*, 81–99. [[CrossRef](#)]
48. Boudda, A.; Choubert, G.; Faure-Muret, A. Essai de stratigraphie de la couverture sédimentaire de l’Anti-Atlas: Adoudounien–Cambrien inférieur. *Notes Mem. Serv. Géol. Maroc.* **1979**, *271*, 96p.
49. Chazan, W. Les gisements stratiformes plombozincifères de l’Infracambrien de l’Anti-Atlas occidental (Maroc). *Notes Mem. Serv. Géol. Maroc.* **1954**, *120*, 97–126.
50. Chbani, B.; Beauchamp, J.; Algouti, A.; Zouhair, A. Eocambrian sedimentary record in a distensional and intracontinental basin: The cycle “basal conglomerates–limestones unit–Tikirt sandstones” of the Bou-Azzer El Graara area (central Anti-Atlas, Morocco). *C. R. Geosci.* **1999**, *329*, 317–323. [[CrossRef](#)]
51. Algouti, A.; Algouti, A.; Beauchamp, J.; Chbani, B.; Taj-Eddine, K. Paléogéographie d’une plateforme infracambrienne en dislocation: Série de base adoudounienne de la région Waoufengha–Igherm, Anti-Atlas occidental, Maroc. *C. R. Acad. Sci.* **2000**, *330*, 155–160. [[CrossRef](#)]
52. Ducrot, J.; Lancelot, J.R. Problème de la limite Précambrien–Cambrien: Étude radiochronologique par la méthode U–Pb sur zircons du volcan du Jbel Boho (Anti-Atlas marocain). *Can. J. Earth Sci.* **1977**, *14*, 2771–2777. [[CrossRef](#)]
53. Gasquet, D.; Levresse, G.; Cheilletz, A.; Azizi-Samir, M.R.; Mouttaqi, A. Contribution to a geodynamic reconstruction of the Anti-Atlas (Morocco) during Pan-African times with the emphasis on inversion tectonics and metallogenic activity at the Precambrian–Cambrian transition. *Precambrian Res.* **2005**, *140*, 157–182. [[CrossRef](#)]
54. Benssaou, M.; Hamoumi, N. Stratigraphic and environmental significance of the Lower-Cambrian western Anti-Atlasic microbialites (Morocco). *C. R. Geosci.* **2004**, *336*, 109–116. [[CrossRef](#)]
55. Benziane, F.; Yazidi, A.; Prost, A.E. Le passage du précambrien, le Cambrien précoce volcanique et sédimentaire de l’Anti-Atlas oriental, comparaisons avec l’Anti-Atlas occidental. *Bull. Soc. Géol. Fr.* **1983**, *7*, 549–556. [[CrossRef](#)]
56. Álvaro, J.J.; Benziane, F.; Thomas, R.; Walsh, G.J.; Yazidi, A. Neoproterozoic–Cambrian stratigraphic framework of the Anti-Atlas and Ouzellagh promontory (High Atlas), Morocco. *J. Afr. Earth Sci.* **2014**, *98*, 19–33. [[CrossRef](#)]
57. Destombes, S.; Hollard, H.; Willefert, S. Lower palaeozoic rocks of Morocco. In *Proceedings of the Lower Palaeozoic of North-Western and West-Central Africa*; Holland, C.H., Ed.; John Wiley & Sons Ltd.: Hoboken, NY, USA, 1985; pp. 91–336.
58. Geyer, G. Late Precambrian to early Middle Cambrian lithostratigraphy of southern Morocco. *Beringeria* **1989**, *1*, 115–143.
59. Buggisch, W.; Siegert, R. Paleogeography and facies of the ‘grès terminaux’ (uppermost Lower Cambrian, Anti-Atlas/Morocco). In *The Atlas System of Morocco*; Jacobshagen, V.H., Ed.; Springer: Berlin/Heidelberg, Germany, 1988; pp. 107–121. [[CrossRef](#)]
60. Marante, A. Architecture et dynamique des systèmes sédimentaires silico-clastiques sur la “Plate-Forme Géante” Nord-Gondwaniennne: L’Ordovicien Moyen de l’Anti-Atlas Marocain. Ph.D. Thesis, Université Michel Montaigne Bordeaux 3, Bordeaux, France, 2008.
61. Hollard, H. Tableaux de corrélations du Silurien et du Dévonien de l’Anti-Atlas. *Notes Serv. Géol. Maroc* **1981**, *42*, 23.
62. Wendt, J. Disintegration of the continental margin of northwestern Gondwana: Late Devonian of the eastern Anti-Atlas (Morocco). *Geology* **1985**, *13*, 815–818. [[CrossRef](#)]
63. Piqué, A.; Michard, A. Moroccan Hercynides; a synopsis; the Paleozoic sedimentary and tectonic evolution at the northern margin of West Africa. *Am. J. Sci.* **1989**, *289*, 286–330. [[CrossRef](#)]

64. Piqué, A.; Dahmani, M.; Jeannette, D.; Bahi, L. Permanence of structural lines in Morocco from Precambrian to present. *J. Afr. Earth Sci.* **1987**, *6*, 247–256. [[CrossRef](#)]
65. Soulaïmani, A. Interactions Socle/Couverture dans l'Anti-Atlas Occidental (Maroc): Rifting Fini-Protérozoïque et Orogenèse Hercynienne. Ph.D. Thesis, Caddi Ayyad University, Marrakech, Morocco, 1998.
66. Jeannette, D.; Benziane, F.; Yazidi, A. Lithostratigraphie et datation du Protérozoïque de la boutonnière d'Ifni (Anti-Atlas, Maroc). *Precambrian Res.* **1981**, *14*, 363–378. [[CrossRef](#)]
67. Raddi, Y.; Baidder, L.; Tahiri, M.; Michard, A. Variscan deformation at the northern border of the West African Craton, eastern Anti-Atlas, Morocco: Compression of a mosaic of tilted blocks. *Bull. Soc. Geol. Fr.* **2007**, *178*, 343–352. [[CrossRef](#)]
68. Marzoli, A.; Renne, P.R.; Piccirillo, E.M.; Ernesto, M.; Bellieni, G.; Min, A. Extensive 200-million-year-old continental flood basalts of the Central Atlantic Magmatic Province. *Science* **1999**, *284*, 616–618. [[CrossRef](#)] [[PubMed](#)]
69. Corso, J.D.; Marzoli, A.; Tateo, F.; Jenkyns, H.C.; Bertrand, H.; Youbi, N.; Mahmoudi, A.; Font, E.; Buratti, N.; Cirilli, S. The dawn of CAMP volcanism and its bearing on the end-Triassic carbon cycle disruption. *J. Geol. Soc.* **2014**, *171*, 153–164. [[CrossRef](#)]
70. Malusa, M.G.; Polino, R.; Feroni, A.C.; Ellero, A.; Ottria, G.; Baidder, L.; Musumeci, G. Post-Variscan tectonics in eastern anti-atlas (Morocco). *Terra Nova* **2007**, *19*, 481–489. [[CrossRef](#)]
71. Begg, G.C.; Shlonsky, J.A.M.; Arndt, N.T.; Griffin, W.L.; O'Reilly, S.Y.; Hayward, N. Lithospheric, cratonic and geodynamic setting of Ni–Cu–PGE sulfide deposits. *Econ. Geol.* **2010**, *105*, 1057–1070. [[CrossRef](#)]
72. Teson, E.; Teixell, A. Sequence of thrusting and syntectonic sedimentation in the eastern Sub-Atlas thrust belt (Dades and Mgoun valleys, Morocco). *Int. J. Earth Sci.* **2008**, *97*, 103–113. [[CrossRef](#)]
73. Tesón, E.; Pueyo, E.L.; Teixell, A.; Barnolas, A.; Agustí, J.; Furió, M. Magnetostratigraphy of the Ouarzazate Basin: Implications for the timing of deformation and mountain building in the High Atlas Mountains of Morocco. *Geodin. Acta* **2010**, *23*, 151–165. [[CrossRef](#)]
74. Fekkak, A.; Ouanaïmi, H.; Michard, A.; Soulaïmani, A.; Ettachfini, E.M.; Berrada, I.; El Arabi, H.; Lagnaoui, A.; Saddiqi, O. Thick-skinned tectonics in a Late Cretaceous–Neogene intracontinental belt (High Atlas Mountains, Morocco): The flat-ramp fault control on basement shortening and cover folding. *J. Afr. Earth Sci.* **2018**, *140*, 169–188. [[CrossRef](#)]
75. Robert-Charrue, C.; Burkhard, M. Inversion tectonics, interference pattern and extensional fault-related folding in the Eastern Anti-Atlas, Morocco. *Swiss J. Geosci.* **2008**, *101*, 397–408. [[CrossRef](#)]
76. Hassenforder, B. La Tectonique Panafricaine et Varisque de l'Anti-Atlas dans le Massif du Kerdous, Maroc. Ph.D. Thesis, University of Strasbourg, Strasbourg, France, 1987.
77. MEM. Carte géologique du Maroc 1:200.000, Feuille Todrha-Ma'der. *Notes Mém. Serv. Géol. Maroc.* **1988**, n°243.
78. MEM. Carte géologique du Maroc 1:100.000, Feuille Igherm. *Notes Mém. Serv. Géol. Maroc.* **1983**, n°309.
79. MEM. Carte géologique du Maroc 1:100.000, Feuille Tafraout. *Notes Mém. Serv. Géol. Maroc.* **1983**, n°307.
80. MEM. Carte géologique du Maroc 1:200.000, Feuille Zagora-Coude du Dra-Hamada du Dra. *Notes Mém. Serv. Géol. Maroc.* **1989**, n°273.
81. Burbank, D.W.; Anderson, R.S. *Tectonic Geomorphology: A Frontier in Earth Science*; Blackwell Science Ltd.: Oxford, UK, 2001.
82. Cotton, C.A. Tectonic scarps and fault valleys. *Geol. Soc. Am. Bull.* **1950**, *61*, 717–758. [[CrossRef](#)]
83. Wallace, R.E. Geometry and rates of change of fault-generated range fronts, north-central Nevada. *J. Res. US Geol. Surv.* **1978**, *6*, 637–650.
84. Stearns, D.W.; Matthews, V. Faulting and forced folding in the Rocky Mountains foreland. *Geol. Soc. Am. Mem.* **1978**, *151*, 1–38.
85. Asladay, A.; Barodi, E.B.; Maacha, L.; Zinbi, Y. Les minéralisations cuprifères du Maroc. *Chron. Rech. Min.* **1998**, *531–532*, 29–44.
86. Leblanc, M. Sur le style disharmonique des plis hercyniens, a la base de la couverture, dans l'Anti-Atlas central (Maroc). *C. R. Acad. Sci.* **1972**, *275*, 803–806.
87. Burkhard, M.; Caritg, S.; Helg, U.; Robert-Charrue, C.; Soulaïmani, A. Tectonics of the Anti-Atlas of Morocco. *C. R. Geosci.* **2006**, *338*, 11–24. [[CrossRef](#)]
88. Davies, J.; Marzoli, A.; Bertrand, H.; Youbi, N.; Ernesto, M.; Schaltegger, U. End-Triassic mass extinction started by intrusive CAMP activity. *Nat. Commun.* **2017**, *8*, 15596. [[CrossRef](#)] [[PubMed](#)]
89. Emran, A.; Chorowicz, J. La tectonique polyphasée dans la boutonnière précambrienne de Bou Azzer (Anti-Atlas central, Maroc): Apports de l'imagerie spatiale Landsat-MSS et de l'analyse structurale de terrain. *Sci. Géol. Bull.* **1992**, *45*, 121–134.
90. Kharis, A.; Aïssa, M.; Baidder, L.; Ouguir, H.; Mahdoudi, M.L.; Zouhair, M.; Ouadjou, A. Oumjrane-Bou Nahas, une mine de cuivre dans l'Ordovicien supérieur du Maider [Oumjrane-Bou Nahas, a Copper Mine in the Maider Upper Ordovician Quartzites]. In *Nouveaux Guides Géologiques et Miniers du Maroc, Principales Mines du Maroc*; Mouttaqi, A., Rjimati, E.C., Maacha, L., Michard, A., Soulaïmani, A., Ibouh, H., Eds.; Notes et Mémoires du Service Géologique du Maroc; Ministère de l'Énergie, des Mines, de l'Eau et l'Environnement: Rabat, Morocco, 2011; Volume 9, pp. 65–71.
91. Boissavy, C. Etude Structurale et Métallogénique des Filons Cuprifères du Maïder Occidental (Anti-Atlas Marocain). Ph.D. Thesis, Université Pierre et Marie Curie, Paris, France, 1979.
92. Choubert, G. L'accident majeur de l'Anti-Atlas. *C. R. Acad. Sci. Paris* **1947**, *224*, 1172–1173.
93. Baidder, L.; Raddi, Y.; Tahiri, M.; Michard, A. Devonian extension of the Pan-African crust north of the West African craton, and its bearing on the Variscan foreland deformation: Evidence from eastern Anti-Atlas (Morocco). *Geol. Soc. Lond. Spec. Publ.* **2008**, *297*, 453–465. [[CrossRef](#)]

94. Bouchta, R.; Boyer, F.; Routhier, P.; Saadi, M.; Salem, M. L'aire cuprifère de l'Anti-Atlas (Maroc); permanence et arêtes riches. *C.R. Acad. Sc. Paris* **1977**, *284*, 503–506.
95. Echogdali, F.Z.; Boutaleb, S.; Abia, E.H.; Ouchchen, M.; Dadi, B.; Id-Belqas, M.; Abioui, M.; Pham, L.T.; Abu-Alam, T.; Mickus, K.L. Mineral prospectivity mapping: A potential technique for sustainable mineral exploration and mining activities—A case study using the copper deposits of the Tagmout basin, Morocco. *Geocarto Int.* **2021**, *37*, 9110–9131. [[CrossRef](#)]
96. Ouchchen, M.; Boutaleb, S.; El Azzab, D.; Abioui, M.; Mickus, K.L.; Miftah, A.; Echogdali, F.Z.; Dadi, B. Structural interpretation of the Igherm region (Western Anti Atlas, Morocco) from an aeromagnetic analysis: Implications for copper exploration. *J. Afr. Earth Sci.* **2021**, *176*, 104140. [[CrossRef](#)]
97. Pham, L.T.; Ouchchen, M.; Eldosouky, A.M.; Boutaleb, S.; Abdelrahman, K.; Gomez-Ortiz, D.; Do, T.D.; Fnais, M.S.; Abioui, M. Reinterpreting aeromagnetic data of the Agadir Melloul region (Morocco) for delineating structural lineaments: A new look. *J. King Saud Univ.* **2022**, *34*, 102325. [[CrossRef](#)]
98. Mamouch, Y.; Attou, A.; Miftah, A.; Ouchchen, M.; Dadi, B.; Moussaid, A.; Et-tayea, Y.; El Azmi, M.; Boualoul, M. Aeromagnetic data of the Kelâat M'Gouna inlier (Jbel Saghro, Eastern Anti-Atlas, Morocco): Geotectonic and mining implications. *J. Afr. Earth Sci.* **2023**, *197*, 104744. [[CrossRef](#)]
99. Ouchchen, M.; Boutaleb, S.; Abia, E.H.; El Azzab, D.; Miftah, A.; Dadi, B.; Echogdali, F.Z.; Mamouch, Y.; Pradhan, B.; Santosh, M.; et al. Exploration targeting of copper deposits using staged factor analysis, geochemical mineralization prospectivity index, and fractal model (Western Anti-Atlas, Morocco). *Ore Geol. Rev.* **2022**, *143*, 104762. [[CrossRef](#)]
100. Miftah, A.; El Azzab, D.; Attou, A.; Ouchchen, M.; Mamouch, Y.; Achkouch, L.; Soulaïmani, A.; Soulaïmani, S.; Manar, A. Mapping of favourable mining areas in the Tiouit area by multispectral remote sensing and airborne gamma-ray spectrometry coupled with geochemical data (Eastern Anti-Atlas, Morocco). *Appl. Earth Sci.* **2022**, *131*, 149–166. [[CrossRef](#)]
101. Mamouch, Y.; Attou, A.; Miftah, A.; Ouchchen, M.; Dadi, B.; Achkouch, L.; Et-tayea, Y.; Allaoui, A.; Boualoul, M.; Randazzo, G.; et al. Mapping of Hydrothermal Alteration Zones in the Kelâat M'Gouna Region Using Airborne Gamma-Ray Spectrometry and Remote Sensing Data: Mining Implications (Eastern Anti-Atlas, Morocco). *Appl. Sci.* **2022**, *12*, 957. [[CrossRef](#)]
102. Abia, E.H.; Soulaïmani, A. Les filons de quartz à oligiste de l'Anti-Atlas central [The Hematite-rich Quartz Veins of Central Anti-Atlas]. In *Nouveaux Guides Géologiques et Minières du Maroc, Principales Mines du Maroc*; Mouттаqi, A., Rjimati, E.C., Maacha, L., Michard, A., Soulaïmani, A., Ibouh, H., Eds.; Notes et Mémoires du Service Géologique du Maroc; Ministère de l'Energie, des Mines, de l'Eau et l'Environnement: Rabat, Morocco, 2011; Volume 9, pp. 129–1131.
103. Oukassou, M.; Saddiqi, O.; Barbarand, J.; Sebti, S.; Baidder, L.; Michard, A. Post-Variscan exhumation of the Central Anti-Atlas (Morocco) constrained by zircon and apatite fission-track thermochronology. *Terra Nova* **2013**, *25*, 151–159. [[CrossRef](#)]
104. Ruiz, G.; Sebti, S.; Saddiqi, O.; Negro, F.; de Lamotte, D.F.; Stockli, D.; Foeken, J.; Stuart, F.; Barbarand, J. Mesozoic to recent denudation patterns in the Anti-Atlas of SW Morocco. *Terra Nova* **2010**, *23*, 35–41. [[CrossRef](#)]
105. Tahir, Y.; Rziki, S.; Soror, T.; Sellami, M.; Benhachemi, M.K. Exploitation d'une mine à ciel ouvert au-dessus et à travers les vides d'une ancienne exploitation souterraine: Cas de la mine à ciel ouvert de cuivre de Tazalaght [Operate an open pit over and through the voids of an old underground mining: Case of Tazalaght copper Ore open pit mine]. *Int. J. Innov. Appl. Stud.* **2016**, *14*, 37–45.
106. Marzoli, A.; Bertrand, H.; Youbi, N.; Callegaro, S.; Merle, R.; Reisberg, L.; Chiaradia, M.; Brownlee, S.I.; Jourdan, F.; Zanetti, A. The Central Atlantic Magmatic Province (CAMP) in Morocco. *J. Petrol.* **2019**, *60*, 945–996. [[CrossRef](#)]
107. Schlische, R.W. Geometry and origin of fault-related folds in extensional settings. *AAPG Bull.* **1995**, *79*, 1661–1678. [[CrossRef](#)]
108. Khalil, S.M.; McClay, K.R. Extensional fault-related folding, northwestern Red Sea, Egypt. *J. Struct. Geol.* **2002**, *24*, 743–762. [[CrossRef](#)]
109. Withjack, M.O.; Olson, J.; Peterson, E. Experimental models of extensional forced folds. *AAPG Bull.* **1990**, *74*, 1038–1054. [[CrossRef](#)]
110. Hardy, S.; McClay, K. Kinematic modelling of extensional fault-propagation folding. *J. Struct. Geol.* **1999**, *21*, 695–702. [[CrossRef](#)]
111. Finch, E.; Hardy, S.; Gawthorpe, R. Discrete-element modelling of extensional fault-propagation folding above rigid basement fault blocks. *Basin Res.* **2004**, *16*, 467–488. [[CrossRef](#)]
112. Erslev, E.A. Trishear fault-propagation folding. *Geology* **1991**, *19*, 617–620. [[CrossRef](#)]
113. Petit, J.P.; Proust, F.; Tapponnier, P. Sens et grandeur des rejets, et axes de la déformation dans la zone de décrochement du Tizi n'Test (Maroc) depuis le Carbonifère. In *Réunion Annuelle des Sciences de la Terre*; Société Géologique de France: Montpellier, France, 1975; p. 291.
114. Poot, J.; Verhaert, M.; Dekoninck, A.; Oummouch, A.; El Basbas, A.; Maacha, L.; Yans, J. Characterization of weathering processes of the giant copper deposit of Tizert (Igherm inlier, anti-atlas, Morocco). *Minerals* **2020**, *10*, 620. [[CrossRef](#)]

Disclaimer/Publisher's Note: The statements, opinions and data contained in all publications are solely those of the individual author(s) and contributor(s) and not of MDPI and/or the editor(s). MDPI and/or the editor(s) disclaim responsibility for any injury to people or property resulting from any ideas, methods, instructions or products referred to in the content.